

4

AD-A214 958

VELOCITY PROFILE AND WALL SHEAR STRESS  
MEASUREMENTS FOR A  
LARGE EDDY BREAK-UP DEVICE (LEBU)

by

DTIC FILE COPY

KURT W. ROTH and PATRICK LEEHEY

Report No. 71435-1  
November, 1989

DTIC  
ELECTE  
DEC 04 1989  
S E D

Acoustics and Vibration Laboratory

DISTRIBUTION STATEMENT A  
Approved for public release;  
Distribution Unlimited

89 11 23 089

REPORT DOCUMENTATION PAGE

1a REPORT SECURITY CLASSIFICATION <b>Unclassified</b>		1b RESTRICTIVE MARKINGS	
2a SECURITY CLASSIFICATION AUTHORITY		3 DISTRIBUTION AVAILABILITY OF REPORT Approved for Public Release. Distribution unlimited.	
2b DECLASSIFICATION/DOWNGRADING SCHEDULE			
4 PERFORMING ORGANIZATION REPORT NUMBER(S) Acoustics and Vibrations Laboratory Report 71435-1		5 MONITORING ORGANIZATION REPORT NUMBER(S)	
6a NAME OF PERFORMING ORGANIZATION Massachusetts Institute of Technology	6b OFFICE SYMBOL (if applicable)	7a. NAME OF MONITORING ORGANIZATION Office of Naval Research, Code 1215	
6c ADDRESS (City, State, and ZIP Code) Cambridge, MA 02139		7b ADDRESS (City, State, and ZIP Code) 800 North Quincy Street Arlington, VA 22217-5000	
8a NAME OF FUNDING / SPONSORING ORGANIZATION Office of Naval Research	8b OFFICE SYMBOL (if applicable) Code 1215	9 PROCUREMENT INSTRUMENT IDENTIFICATION NUMBER N00014-89-J-1176	
8c ADDRESS (City, State, and ZIP Code) 800 North Quincy Street Arlington, VA 22217-5000		10 SOURCE OF FUNDING NUMBERS	
		PROGRAM ELEMENT NO	PROJECT NO
		TASK NO	WORK UNIT ACCESSION NO
11 TITLE (Include Security Classification) Velocity Profile and Wall Shear Stress Measurements for a Large Eddy Breakup Device (LEBU)			
12 PERSONAL AUTHOR(S) K. W. Roth and P. Lechey			
13a TYPE OF REPORT Technical	13b TIME COVERED FROM _____ TO _____	14 DATE OF REPORT (Year, Month, Day) 1989 November 2	15 PAGE COUNT 59
16 SUPPLEMENTARY NOTATION			
17 COSATI CODES		18 SUBJECT TERMS (Continue on reverse if necessary and identify by block number)	
FIELD	GROUP	Boundary layer manipulation: Wall shear stress reduction. <i>Flow separation study</i>	
	SUB-GROUP		
19 ABSTRACT (Continue on reverse if necessary and identify by block number)			
<p>Wind tunnel experiments were performed in the M.I.T. Acoustics &amp; Vibrations Laboratory to determine the reduction in mean wall shear stress achieved by honeycomb matrix Large Eddy Break-Up Device (LEBU) and study how such a device alters a turbulent boundary layer.</p> <p>The LEBUs considered significantly altered the steady and unsteady velocity components, and moved the active region of the boundary layer further from the wall.</p> <p>The LEBUs studied achieved at least a 10% reduction of mean wall shear stress for distances over 300 displacement thicknesses behind the device. The LEBU parameter of height was found to affect the level and duration of mean wall shear stress reduction. Surface fence measurements indicated that the boundary layer manipulated by the LEBU does not adhere to the Coles "Law of the Wall", possessing a large "B" intercept.</p>			
20 DISTRIBUTION AVAILABILITY OF ABSTRACT <input checked="" type="checkbox"/> UNCLASSIFIED/UNLIMITED <input type="checkbox"/> SAME AS RPT <input type="checkbox"/> DTIC USERS		21 ABSTRACT SECURITY CLASSIFICATION <b>Unclassified</b>	
22a NAME OF RESPONSIBLE INDIVIDUAL Patrick Lechey		22b TELEPHONE (Include Area Code) (617) 253-4337	OFFICE SYMBOL Room 3-262

VELOCITY PROFILE AND WALL SHEAR STRESS  
MEASUREMENTS FOR A  
LARGE EDDY BREAK-UP DEVICE (LEBU)

by

Kurt W. Roth and Patrick Leehey

ABSTRACT

Wind tunnel experiments were performed in the M.I.T. Acoustics & Vibrations Laboratory to determine the reduction in mean wall shear stress achieved by honeycomb matrix Large Eddy Break-Up Device (LEBU) and study how such a device alters a turbulent boundary layer.

The LEBUs considered significantly altered the steady and unsteady velocity components, and moved the active region of the boundary layer further from the wall.

The LEBUs studied achieved at least a 10% reduction of mean wall shear stress for distances over 300 displacement thicknesses behind the device. The LEBU parameter of height was found to affect the level and duration of mean wall shear stress reduction. Surface fence measurements indicated that the boundary layer manipulated by the LEBU does not adhere to the Coles "Law of the Wall", possessing a larger "B" intercept.

Accession For	
NTIS GRA&I	<input checked="" type="checkbox"/>
DTIC TAB	<input type="checkbox"/>
Unannounced	<input type="checkbox"/>
Justification	
By _____	
Distribution/	
Availability Codes	
Dist	Avail and/or Special
A-1	



### ACKNOWLEDGEMENTS

Support for this work was provided by the Office of Naval Research, Codes 1215 and 11250A, and the David Taylor Research Center, Code 1942. An instrumentation grant was also provided by the Sea Grant Program at M.I.T.

TABLE OF CONTENTS

	page
Abstract	2
Acknowledgements	3
Table of Contents	4
Nomenclature	5
List of Figures	6
1. Introduction	8
1.1 Introduction	8
1.2 Objectives	9
2. Experiment Description	9
2.1 The Device	9
2.2 The Tunnel and Test Plate	10
2.3 Velocity Measurements	12
2.4 Wall Shear Measurements	13
3. Experimental Results	15
3.1 Velocity Profiles Produced by a LEBU	15
3.1.1 Mean Velocity	15
3.1.2 Fluctuating Velocity	16
3.2 Wall Shear Stress Reduction Achieved by a LEBU	17
3.3 The LEBU and Coles "Law of the Wall"	18
4. Conclusions	20
Bibliography	21

NOMENCLATURE

$Cf_{manip}$	Manipulated Skin Friction Coefficient
$Cf_{unmanip}$	Unmanipulated Skin Friction Coefficient
D	LEBU Cell Diameter
$dP_{fence}$	Pressure Drop Across Sublayer Surface Fence
$\frac{dp}{dx}$	Pressure Gradient Along Test Plate
H	LEBU Height
h+	Height of Sublayer Surface Fence in Viscous Units
L	LEBU Streamwise Length
$Re_{fence}$	Reynolds Number Based on Sublayer Surface Fence Height
$\bar{U}$	Mean Flow Velocity
$U_{\infty}$	Freestream Velocity of Flow
$u'$	Root Mean Square (RMS) Fluctuating Velocity Component
u+	Mean Velocity in Viscous Units
$u_{\tau}$	Friction Velocity, $\sqrt{\frac{\tau_w}{\rho}}$
$x_{LEBU}$	Distance Behind LEBU
y	Distance From Wall
y+	Distance From Wall in Viscous Units
$\delta^*_{inc}$	Incident Displacement Thickness at LEBU
$\nu$	Kinematic Viscosity
$\rho$	Density of Air
$\tau_w$	Mean Wall Shear Stress

LIST OF FIGURES

	page
1. Diagram of Honeycomb LEBU	22
2. Wind Tunnel Facility	23
3. Diagram of Surface Fence	24
4. Hotwire Traverse	25
5a. Unmanipulated Coles Plot, $y^+$ vs. $u^+$ , $U_\infty = 5 \frac{m}{s}$ , $x_{LEBU} = 16.5in.$	26
5b. Unmanipulated Coles Plot, $y^+$ vs. $u^+$ , $U_\infty = 35 \frac{m}{s}$ , $x_{LEBU} = 16.5in.$	27
6a. Unmanipulated Profile, $\bar{U}$ vs. $y$ , $x_{LEBU} = 0in.$ , $U_\infty = 15 \frac{m}{s}$ .	28
6b. Unmanipulated Profile, $\bar{U}$ vs. $y$ , $x_{LEBU} = 5in.$ , $U_\infty = 15 \frac{m}{s}$ .	29
6c. Unmanipulated Profile, $\bar{U}$ vs. $y$ , $x_{LEBU} = 10in.$ , $U_\infty = 15 \frac{m}{s}$ .	30
6d. Unmanipulated Profile, $\bar{U}$ vs. $y$ , $x_{LEBU} = 15in.$ , $U_\infty = 15 \frac{m}{s}$ .	31
6e. Unmanipulated Profile, $\bar{U}$ vs. $y$ , $x_{LEBU} = 20in.$ , $U_\infty = 15 \frac{m}{s}$ .	32
6f. Unmanipulated Profile, $\bar{U}$ vs. $y$ , $x_{LEBU} = 25in.$ , $U_\infty = 15 \frac{m}{s}$ .	33
7a. Manipulated Profile, $\bar{U}$ vs. $y$ , $6 - \frac{1}{8}$ in.cells LEBU, $x_{LEBU} = 1in.$ , $U_\infty = 14 \frac{m}{s}$ .	34
7b. Manipulated Profile, $\bar{U}$ vs. $y$ , $6 - \frac{1}{8}$ in.cells LEBU, $x_{LEBU} = 3in.$ , $U_\infty = 14 \frac{m}{s}$ .	35
7c. Manipulated Profile, $\bar{U}$ vs. $y$ , $6 - \frac{1}{8}$ in.cells LEBU, $x_{LEBU} = 5in.$ , $U_\infty = 14 \frac{m}{s}$ .	36
7d. Manipulated Profile, $\bar{U}$ vs. $y$ , $6 - \frac{1}{8}$ in.cells LEBU, $x_{LEBU} = 10in.$ , $U_\infty = 14 \frac{m}{s}$ .	37
7e. Manipulated Profile, $\bar{U}$ vs. $y$ , $6 - \frac{1}{8}$ in.cells LEBU, $x_{LEBU} = 15in.$ , $U_\infty = 14 \frac{m}{s}$ .	38
7f. Manipulated Profile, $\bar{U}$ vs. $y$ , $6 - \frac{1}{8}$ in.cells LEBU, $x_{LEBU} = 25in.$ , $U_\infty = 14 \frac{m}{s}$ .	39
7g. Manipulated Profile, $\bar{U}$ vs. $y$ , $6 - \frac{1}{8}$ in.cells LEBU, $x_{LEBU} = 35in.$ , $U_\infty = 14 \frac{m}{s}$ .	40

8a. Unmanipulated Profile, $u'$ vs. $y$ , $x_{LEBU} = 0in.$ , $U_{\infty} = 15 \frac{m}{s}$	41
8b. Unmanipulated Profile, $u'$ vs. $y$ , $x_{LEBU} = 5in.$ , $U_{\infty} = 15 \frac{m}{s}$	42
8c. Unmanipulated Profile, $u'$ vs. $y$ , $x_{LEBU} = 10in.$ , $U_{\infty} = 15 \frac{m}{s}$	43
8d. Unmanipulated Profile, $u'$ vs. $y$ , $x_{LEBU} = 15in.$ , $U_{\infty} = 15 \frac{m}{s}$	44
8e. Unmanipulated Profile, $u'$ vs. $y$ , $s_{LEBU} = 25in.$ , $U_{\infty} = 15 \frac{m}{s}$	45
9a. Manipulated Profile, $u'$ vs. $y$ , $6 - \frac{1}{8}$ in. cells LEBU, $x_{LEBU} = 1in.$ , $U_{\infty} = 14 \frac{m}{s}$	46
9b. Manipulated Profile, $u'$ vs. $y$ , $6 - \frac{1}{8}$ in. cells LEBU, $x_{LEBU} = 3in.$ , $U_{\infty} = 14 \frac{m}{s}$	47
9c. Manipulated Profile, $u'$ vs. $y$ , $6 - \frac{1}{8}$ in. cells LEBU, $x_{LEBU} = 5in.$ , $U_{\infty} = 14 \frac{m}{s}$	48
9d. Manipulated Profile, $u'$ vs. $y$ , $6 - \frac{1}{8}$ in. cells LEBU, $x_{LEBU} = 10in.$ , $U_{\infty} = 14 \frac{m}{s}$	49
9e. Manipulated Profile, $u'$ vs. $y$ , $6 - \frac{1}{8}$ in. cells LEBU, $x_{LEBU} = 15in.$ , $U_{\infty} = 14 \frac{m}{s}$	50
9f. Manipulated Profile, $u'$ vs. $y$ , $6 - \frac{1}{8}$ in. cells LEBU, $x_{LEBU} = 25in.$ , $U_{\infty} = 14 \frac{m}{s}$	51
9g. Manipulated Profile, $u'$ vs. $y$ , $6 - \frac{1}{8}$ in. cells LEBU, $x_{LEBU} = 45in.$ , $U_{\infty} = 14 \frac{m}{s}$	52
10a. Cf Reduction, $3 - \frac{1}{8}$ in. cells LEBU, $\frac{Cf_{man}}{Cf_{unman}}$ vs. $\frac{x_{LEBU}}{\delta^*_{inc}}$	53
10b. Cf Reduction, $6 - \frac{1}{8}$ in. cells LEBU, $\frac{Cf_{man}}{Cf_{unman}}$ vs. $\frac{x_{LEBU}}{\delta^*_{inc}}$	54
10c. Cf Reduction, $9 - \frac{1}{8}$ in. cells LEBU, $\frac{Cf_{man}}{Cf_{unman}}$ vs. $\frac{x_{LEBU}}{\delta^*_{inc}}$	55
11. Surface Fence Calibration, $\log_{10} dP_{fence}$ vs. $\log_{10} \tau_w$	56
12a. Manipulated Coles Plot, Surface Fence $\tau_w$ , $y+$ vs. $u+$ , $U_{\infty} = 26 \frac{m}{s}$	57
12b. Manipulated Coles Plot, Surface Fence $\tau_w$ , $y+$ vs. $u+$ , $U_{\infty} = 32 \frac{m}{s}$	58
12c. Manipulated Coles Plot, Surface Fence $\tau_w$ , $y+$ vs. $u+$ , $U_{\infty} = 37 \frac{m}{s}$	59



## 1. INTRODUCTION

### 1.1. Background

Much research has been recently performed to study how a Large Eddy Break-Up device (LEBU) can be used to manipulate a turbulent boundary layer. The primary focus of most LEBU studies has been a reduction in the skin friction coefficient downstream of the device. Although LEBUs have definitely achieved significant local reductions in skin friction, measurements have generally shown that a LEBU does not obtain an overall reduction in drag.

Another possible application of the LEBU would be to reduce the fluctuating wall pressures that a turbulent boundary layer produces. It has been shown that fluctuating wall pressure scales with the mean wall shear stress, so that a reduction in wall shear stress would indicate a reduced fluctuating wall pressure. The function of a LEBU is to break the larger structures of a turbulent boundary layer into smaller vortices, and it is hypothesized that these larger eddy structures are primarily responsible for inducing low wavenumber fluctuating wall pressures [1].

Therefore, LEBUs show considerable promise for reducing fluctuating wall pressures.

However, not much is known about how a LEBU alters a turbulent boundary layer and its structures. The experiments detailed herein present an in-depth study of how a LEBU alters a turbulent boundary layer and reduces the wall shear stress.

### 1.2. Objectives

The central goals of the research were: 1) to design the most effective LEBU to reduce wall shear stress, 2) to measure how a LEBU alters the steady and fluctuating components of the velocity profile of a turbulent boundary layer, and the streamwise extent to which the effect of the

---

1. Bradshaw, P. (1967), "'Inactive' Motion and Pressure Fluctuations in Turbulent Boundary Layers", J. Fluid Mechanics, vol. 30, part 2, pp. 241-258.

LEBU persists, 3) to quantify the reduction in wall shear stress produced by a LEBU, and 4) to determine if the Coles "Law of the Wall" applies to the non-equilibrium boundary layer created by a LEBU.

-----

## 2. EXPERIMENT DESCRIPTION

### 2.1. The Device

Aluminum honeycomb matrices with several different heights, cell diameters, and stream-wise lengths were used to manipulate a turbulent boundary layer (Figure 1). The past success of honeycomb matrices in reducing wall shear and the skin friction coefficient motivated the use of honeycomb as a LEBU. Initially, tests were performed using the same LEBU as Moller and Leehey [2] : 1" high, 1/4" cell diameter, and 2" long at the base tapering to 1/2" at the top. Ultimately, six new LEBU designs were built and tested to try to optimize wall shear reduction.

As mentioned earlier, a basic knowledge of how a LEBU reduces wall shear stress does not exist. A fundamental question that was explored was to determine if a LEBU achieved a reduction in wall shear stress by primarily altering the inner "wall" region of the boundary layer or the outer "wake" region. To address this issue, four LEBUs were constructed with identical stream-wise lengths,  $L = 1$ ", and cell diameters,  $D = 1/8$ ", but different heights:  $H = 0.375$ ",  $0.75$ ",  $1$ ", and  $1.125$ ".

The parameter of cell diameter was also considered important because it would reflect the scale of turbulent structures that the LEBU was altering. For example, a LEBU with a smaller cell diameter would most likely "break" the turbulent structures into smaller vortices which

2. Moller, James Christian and Partick Leehey, "Measurement of Wall Shear and Pressure Downstream of a Honeycomb Boundary Layer Manipulator". M.I.T. Acoustics and Vibration Laboratory Report no. 97457-3, April, 1989.

would then take longer to regenerate into the larger eddy structures which are thought to be the primary cause of fluctuating wall pressures. On the other hand, a LEBU with too small a cell diameter would tend to behave similarly to a wall placed in the flow and cause the airflow to flow over the LEBU, separate from the top of the LEBU, and reattach downstream of the device. The separation and reattachment scenario clearly is not desirable, as at reattachment the flow would impinge upon the the plate and expose the plate to pressures far greater than those induced by a turbulent boundary layer [3]. Two LEBU's with essentially the same height but different cell diameters, 1/4" and 1/8", were constructed and tested to determine a general trend in cell diameter for more effective LEBU design. The LEBU streamwise length was also altered to see if a greater length would enhance wall shear reduction.

The thickness of the turbulent boundary layer just before it passed through the LEBU was approximately 0.8 inches and varied slightly with the freestream velocity,  $U_{\infty}$ .

## 2.2. The Tunnel and Test Plate

All of the tests were performed in the low-turbulence, low-noise wind tunnel of the M.I.T. Acoustics and Vibration Laboratory (Figure 2) Free stream turbulence levels,  $\frac{u'}{U_{\infty}}$ , of from 0.05 to 0.08% were measured. The tunnel was constructed and documented by Hanson [4], and is presently driven by a General Electric Model DC-300 blower motor. The tests were carried out with tunnel set up in a closed duct configuration. The tunnel test cross-section is 15" by 15".

A plexiglass plate, 15" wide and 100" long was constructed to perform tests. The leading edge of the plexiglass plate was sanded into a semi-ellipse with an aspect ratio of approximately 6:1 to prevent flow separation from occurring there [5]. The plate was mounted at 56" from the entrance into the test section sloping down towards the back of the tunnel at an angle of one

3. Farabee, T. M. (1986), "An Experimental Investigation of Wall Pressure Fluctuations Beneath Non-Equilibrium Turbulent Flows". DTNSRDC-86/047.

4. Hanson, C.E. (1969), "The Design and Construction of a Low Noise, Low Turbulence Wind Tunnel", Acoustics and Vibration Laboratory M.I.T. Report no. 79611-1.

5. Shapiro, Paul J., "The Influence of Sound Upon Laminar Boundary Layer Instability", M.I.T. Acoustics & Vibrations Laboratory Report no. 83458-83560-1, Sept., 1977.

degree. This resulted in the plate resting 9" below the top of the tunnel wall at the front and 10" from the top tunnel wall at its end. An adjustable aluminum flap was bolted to the back of the plate and used to obtain a zero pressure gradient along the plate. Two pressure taps, placed over 50" apart and leading to a Validyne Model CD23 pressure transducer calibrated against a Betz manometer, were used to verify that  $\frac{dp}{dx} = 0$  along the plate. The plate was mounted on two aluminum rails, with damping material placed between the rails and the plate to minimize vibration. The rails were in turn attached by bolts to the wall of the tunnel. In preparation for the tests, all tunnel joints were filled with wood putty, and sanded smooth with 320 grit sand paper.

All of the LEBUs were mounted at a distance of 35" from the leading edge of the plate using a silicon rubber cement adhesive. The surface fence (Figure 3) was inserted in the plate approximately 51.5" from the leading edge, or 16.5" behind the LEBU. The circular top surface of the surface fence was mounted flush with the plexiglass test plate by pushing the top of the gage up against a small ruler that was held flush with the test plate. After the circular top of the surface fence was flush with the top of the test plate, a screw mounted on the bottom of the test plate was tightened to hold the fence in place. The small gap between the circular top of the surface fence and the test plate was filled with putty and smoothed to prevent a suction from developing around the outside edge of the circular top of the surface fence. A two-inch wide strip of 30 grit sandpaper was attached 10" from the leading edge of the plate to trip the flow and create a turbulent boundary layer. Tests were carried out at several different freestream velocities ranging from 5 m/s to 35 m/s.

### 2.3. Velocity Measurements

A hotwire traverse was used to acquire all velocity data (Figure 4). The traverse runs on tracks mounted to the wind tunnel, and is driven in the streamwise direction by a motor. The sensitivity of the traverse in the x-direction is 0.05 inches. A second motor drives the traverse in the y-direction. A hotwire probe, a TSI 1218-T1.S Model, is mounted to an arm attached to the traverse and can be moved up and in the y-direction via a screw mechanism with a sensitivity of

0.0005 inches. The arm passes through a padded slit, and into the wind tunnel. To prevent vortex shedding off the arm an aluminum cowling covers the probe arm.

The hotwire probe was balanced by a DanTec Model 56C01/17 Constant Temperature Anemometer, and calibrated against a pitot-static probe placed in the potential flow core. The pressure transducer for the pitot-static probe, a Validyne CD23 Model, had been calibrated earlier using a Betz water manometer. To assure an accurate relationship between hotwire voltage and air velocity, the hotwire was calibrated daily using a sixth order curve fit based on at least 15 data points.

A program, "measure.f", was written to automate velocity profile data acquisition on a Masscomp 5400, 32-bit computer. The probe was lowered down to the plate into the buffer region of the boundary layer, and the program controlled the traverse to step the hotwire up through the boundary layer and obtain velocity measurements. The hotwire signal first went through the anemometer, and then was divided into its AC and DC components. The direct current component of the signal passed from the anemometer directly to a 16-channel Analog to Digital converter and then was processed by the data acquisition software on the Masscomp. The AC signal, on the other hand, first passed through an Ithaco 255 amplifier (to better discern the AC magnitude), and was then low-pass filtered at 4kHz by a Krohn-Hite 3550 Model filter. After being displayed on an Nicolette oscilloscope, the AC component of the velocity was converted to a digital signal by the analog to digital converter and reduced by the computer software.

The data acquisition program acquired 80,000 data points at a rate of 20kHz for each measurement to ensure accurate velocity measurements. The program, after acquiring the data, calculated the mean velocity,  $\bar{U}$ , and the root mean squared (RMS) fluctuating velocity,  $u'$ , for each profile point.

## 2.4. Wall Shear Measurements

The wall shear stress,  $\tau_w$ , was obtained using two distinctly different techniques. The first, based on Coles "Law of the Wall" [6], calculated  $\tau_w$  by interpreting velocity profiles, whereas the second technique used a surface fence to measure  $\tau_w$ .

The velocity profile method attempts to fit the data points of the velocity profile to the Coles "Law of the Wall." Using the curve fitting technique is essential in this instance because the hotwire cannot be placed close enough to the wall to obtain velocity data in the viscous sub-layer. Coles assumed that a constant shear layer exists in the boundary layer very near the wall, and that the velocity profile of any type of boundary layer scaled only with  $\tau_w$  and distance from the wall,  $y$ . Coles obtained numerous data points of velocity measurements near the wall which validated this assumption, and created the "law of the wall". The curve fitting technique uses Coles data points, and uses a regression technique to attempt to fit the individual velocity profiles to the Coles data. The program used to perform the regression, "coles.f", calculates the friction velocity,  $u_\tau$ , the  $y$ -offset of the profile from the wall, and the displacement thickness,  $\delta^*$ , of the boundary layer.

The Coles Law has been shown to definitely apply for equilibrium boundary layers, but the validity of the Coles Law in non-equilibrium boundary layers is suspect. Experimental evidence produced by Bradshaw and Wong [7] supports the universality of the "Law of the Wall." However, Kline et. al. [8] discovered that the law did not hold some non-equilibrium flows. The validity of the Coles "Law of the Wall" for the non-equilibrium boundary layer produced by a LEBU was investigated by comparing the  $\tau_w$  arrived at by the Coles curve-fit to the  $\tau_w$  obtained by a second wall shear stress measurement technique, the viscous surface fence.

---

6. Coles, D.E., "The Law of the Wall in Turbulent Shear Flow" *50 Jahre Grenzschichtforschung*, (H. Goertler and W. Tollmien, eds.), F. Vieweg & Sohn, Braunschweig, pp. 153-163.

7. Bradshaw, P. and Wong, F.Y.F., "Reattachment of a Turbulent Shear Layer"(1972), *J. Fluid Mechanics*, vol. 52, pp. 113-135.

8. Kline, S.J., Reynolds, W.C., Schraub, F.A., and Rumstadler, P.W. (1967), "The Structure of Turbulent Boundary Layers", *J. Fluid Mechanics*, vol. 30, part 4, pp. 741-773.

A surface fence was flush-mounted in the plexiglass plate 51.5" from the leading edge or 16.5" behind the LEBU (Figure 3). The surface fence consists of two chambers separated by a narrow plate that protrudes 0.003" into the flow, and is aligned such that the plate is perpendicular to the flow. As the air passes over the plate of the surface fence, the flow separates and a pressure difference develops between the two sides of the plate. The two chambers are attached to a Validyne CD23 Pressure Transducer which reports the pressure drop across the fence. The Validyne signal was low-pass filtered at 4kHz by a Precision Filter Model 32-B-03B-M107 and interpreted by the Masscomp A to D converter and software.

A relationship between wall shear stress and surface fence pressure drop was obtained by carrying out unmanipulated flow experiments and recording the pressure drop across the fence while simultaneously taking a velocity profile of the flow. The velocity profile was then fitted to the Coles "Law of the Wall" using the regression technique to find the corresponding wall shear stress. In this instance use of the Coles fit was justified because an equilibrium boundary layers definitely existed.

The surface fence, as long as it remains in the viscous sublayer ( $h^+ < 10$ ), provides a very accurate measurement of wall shear stress in non-equilibrium boundary layers when compared to a preston tube. The largest  $h^+$  encountered during experiment was  $h^+ = 6$ . Gur and Lechey [9] determined that a surface fence exhibits linear behavior for surface fence heights in viscous units

$$h^+ = \frac{u_\tau h}{\nu}$$

less than 1.6. Since the value of  $h^+$  in our experiment was 6, the the fence produced a non-linear relationship between  $dP_{fence}$  and  $\tau_w$ .

---

9. Gur, Y. and Lechey, P. , Work in progress.

### 3. EXPERIMENTAL RESULTS

#### 3.1. Velocity Profiles Produced by a LEBU

##### 3.1.1. Mean Velocity

The initial mean velocity profiles were of unmanipulated flows (i.e. no LEBU mounted on plate). The unmanipulated profiles were validated by fitting the velocity profiles to the Coles data using the Coles curve-fitting technique already mentioned. Figure 5 shows unmanipulated velocity profiles at low and high Reynolds numbers plotted against the Coles curve. The experimental data agreed very well with the Coles curve. Typical unmanipulated mean velocity profiles for a range of x-positions are presented in Figure 6. All x-positions are referenced to the position of where the LEBU is placed when used, i.e. 35in. from the leading edge of the test plate. For example, an unmanipulated profile at  $x_{LEBU} = 5in.$  represents a profile taken at 40in. from the leading edge of the test plate, which is 5 inches behind where the LEBU would be. This system of nomenclature is used to allow easy comparison of manipulated and unmanipulated velocity profiles.

Figure 7 displays characteristic mean velocity profiles for a manipulated flow at several distances behind a LEBU 3/4" high with a cell diameter of 1/8" at  $U_{\infty} = 14 m/s$ . Figure 7a. shows the mean velocity profile at one inch behind the LEBU,  $x_{LEBU} = 1in.$ . The effect of each individual LEBU cell shows up as a sharp spike in the velocity profile which results from the boundary layer that form in each cell. Three inches behind the LEBU the effects of individual cells can no longer be seen in the mean velocity profiles and the region close to the wall resembles an unmanipulated profile (Figure 7b.). In the outer region of the profile, however, a large inflection persists. The inflection remains discernible at  $x_{LEBU} = 10in.$  (Figure 7d.), until it vanishes almost entirely at  $x_{LEBU} = 15in.$  (Figure 7c.). Clearly, the LEBU alters the outer region of the boundary layer for a longer period than the inner region. The greater duration of the effect of the LEBU in the



outer region relative to the inner region suggests that a primary function of a LEBU is to alter the outer structure of the turbulent boundary layer.

### 3.1.2. Fluctuating Velocity

Figure 8 presents plots of fluctuating velocity,  $u'$ , versus  $y$  for unmanipulated flow at  $U_\infty = 14 \text{ m/s}$ . The greatest turbulence level was found to be  $\frac{u'}{U_\infty} = 8\%$ , and appears as a spike near  $y = 0$ . The turbulence levels encountered near the wall in the high turbulence regions indicate that the hotwire probe was operating in the buffer region of the boundary layer.

The manipulated fluctuating velocity profiles of a LEBU with  $H=0.75''$   $D=0.125''$  in flow with  $U_\infty = 15 \text{ m/s}$  are shown in Figure 9 for several values of  $x_{LEBU}$ . A comparison of unmanipulated and manipulated  $u'$  versus  $y$  plots shows that a LEBU reduces  $\frac{u'}{u_\infty}$  near the wall while increasing  $\frac{u'}{u_\infty}$  in the outer regions of the flow. The increase in outer region turbulence is due to vorticity shed off the individual honeycomb cells and the top of the LEBU. Initially, at  $x_{LEBU} = 1 \text{ in.}$  the shedding from each LEBU cell can be clearly seen (Figure 9a.). At  $x_{LEBU} = 10 \text{ in.}$ , however, the effect of the individual cells upon  $u'$  has disappeared whereas a large wake in the outer region remains (Figure 9d.). The outer wake, which results from shedding off the top of the LEBU, does not disappear until  $x_{LEBU} = 25 \text{ in.}$  (Figure 9f.). The lasting effect the LEBU has upon  $u'$  in the outer layer versus the inner layer parallels the persistence of the effect that the LEBU has upon  $\bar{U}$  in the outer layer relative to near the wall, and further suggests that manipulation of the outer regions of the boundary layer is a primary function of the LEBU.

The higher turbulence levels produced by a LEBU away from the wall also indicates that the LEBU effectively moves the active region of the boundary layer further from the wall. This results in less energy being transported from the potential flow to the wall and may produce the smaller  $u'$  and  $\tau_w$  values of manipulated flow.

### 3.2. Wall Shear Stress Reduction Achieved by a LEBU

The LEBU with  $H=1.125''$  and  $D=0.125''$  was found to achieve the greatest and most enduring reduction in mean wall shear stress. Figure 10 displays local skin friction,  $\frac{Cf_{man}}{Cf_{unman}}$  versus non-dimensional streamwise position  $\frac{x_{LEBU}}{\delta_{*inc}}$  for three LEBUs with  $D=0.125''$  and  $H=0.375'', 0.75'', 1.125''$ . The  $Cf_{unman}$  represents the  $Cf$  value of an unmanipulated flow at the same velocity and  $x$ -position, and was found by a curve fit of 28 unmanipulated  $Cf$  and  $Re_L$  pairs. The incident displacement thickness,  $\delta_{*inc}$ , is the displacement thickness of an unmanipulated boundary layer at the LEBU with freestream velocity  $U_\infty$ . These figures clearly show the importance of the LEBU height in reducing  $Cf$  and wall shear stress. The greatest reduction in  $Cf$  produced by the  $H=0.375''$  and  $H=0.75''$  LEBUs is 45%, whereas the LEBU with  $H=1.125''$  reduces  $Cf$  almost 55%. LEBU height, more importantly, has a profound effect on the streamwise duration of wall shear stress reductions achieved by a LEBU. Arbitrarily defining a skin friction reduction of 10% as significant, a LEBU of  $H=0.375''$  significantly reduces local skin friction for approximately 300 displacement thicknesses (Figure 10a.) and the  $H=0.75''$  LEBU achieves significant reduction at up to  $x_{LEBU} = 500\delta_{*inc}$  (Figure 10b.). The LEBU with  $H=1.125''$  reduces  $Cf$  by at least 30% for all values of  $\frac{x_{LEBU}}{\delta_{*inc}}$  within the scope of the experiment (Figure 10c.). A possible interpretation why the  $H=1.125''$  LEBU  $\frac{Cf_{man}}{Cf_{unman}}$  curve does not converge to one is that the LEBU has the effect of increasing the  $Re_x$  of the flow, which would result in a lower actual  $Cf_{unman}$  value than predicted. The  $Cf$  reduction produced by a honeycomb LEBU was greater in both magnitude and duration than of airfoil LEBUs. Savill [10], using tandem airfoils, obtained a maximum reduction of approximately 15% versus the 45-55% obtained for our 1/8 inch LEBUs. He also noted that the effect of the LEBU was insignificant beyond only 15  $\delta$

10. Savill, A.M.(1987), "On the Manner in Which Outer Layer Disturbances Affect Turbulent Boundary Layer Skin Friction," Advances in Turbulence; Proceedings of the First European Turbulence Conference, Ecully, France, July 1-4, 1986 (A87-52001 23-34). Berlin and New York, Springer-Verlag, pp. 533-545.

compared to a duration of at least  $40 \delta$  for the honeycomb LEBUs we examined. A study of the overall drag reduction of a honeycomb LEBU was not carried out.

The surface fence was also used to measure mean wall shear stress. Figure 11 shows the calibration curve of  $\tau_w$  versus  $dP_{fence}$ , and the relationship between  $\tau_w$  and  $dP_{fence}$  was found to be:

$$\log_{10}\tau_w = .595 \log_{10}dP_{fence} - .572$$

which agrees with the findings of Gur and Leehey. The surface fence measured mean wall shear stress values that were 11% below the  $\tau_w$  found by fitting the manipulated mean velocity profiles to the Coles data.

### 3.3. The LEBU and Coles "Law of the Wall"

The discrepancy in  $\tau_w$  values measured by the surface fence and the Coles curve fit suggests that the Coles' "law of the wall" does not apply in the flow regions manipulated by the LEBU. Plots of  $u^+$  vs.  $y^+$  were made for manipulated flow using  $\tau_w$  measured by the surface fence and the  $y$ -offset calculated by the Coles data fit. Figure 12 shows that the  $u^+$  vs.  $y^+$  plots using  $\tau_w$  of the fence consistently lie above the Coles data plot (solid line), while possessing the same slope. Other researchers have also noted that the Coles "law of the wall" does not hold for the region immediately behind the LEBU, and in each instance, the intercept of the logarithmic region,  $B$ , increased while the slope of the curve remained unchanged. Moller [2], using a honeycomb LEBU, exhibited a value of  $B$  8% greater than predicted by Coles while obtaining the same slope. Drag reduction experiments performed by Savill [10] using tandem airfoil LEBUs also produced  $u^+$  vs.  $y^+$  curves with a 5 to 10% greater  $B$  intercept while possessing the same slope as an unmanipulated boundary layer.

Coles assumed that the mean velocity profile scales only on  $\tau_w$  and the distance from the wall. The discrepancy in  $\tau_w$ , however suggests that the behavior of a boundary layer altered by a LEBU may scale with other parameters, such as cell diameter and LEBU height. For

manipulated and other non-equilibrium boundary layer flows the von Karman slope is preserved but the B intercept is significantly increased. Thus methods for determining mean wall shear stress which depend upon knowledge of the B intercept are unsuitable for such flows. They are conservative, however, in that they overestimate  $\tau_w$  in these circumstances. Therefore, the actual reductions in  $\tau_w$  and Cf achieved by use of LEBUs were greater than as reported in Section 3.2.

-----

#### 4. CONCLUSIONS

1) A LEBU reduces mean wall shear stress and local skin friction coefficient significantly up to at least 300 displacement thicknesses behind the LEBU.

2) The effectiveness of a LEBU, particularly with respect to duration of  $\tau_w$  and  $C_f$  reduction, depends upon the height of the device.

3) A honeycomb LEBU achieves a  $C_f$  reduction far greater than tandem airfoil LEBUs, and the duration of the reduction was significantly longer.

4) The LEBU moves the active region of a turbulent boundary layer further from the wall, reducing the entailment of energy from potential flow to the wall.

5) The boundary layer of a LEBU disagrees with Coles "law of the wall" in the region behind the LEBU, possessing a greater "B" intercept.

## BIBLIOGRAPHY

Bradshaw, P. (1967), "'Inactive' Motion and Pressure Fluctuations in Turbulent Boundary Layers," J. Fluid Mechanics, vol. 30, Part 2, pp. 241-258.

Bradshaw, P. and F.Y.F. Wong (1972), "Reattachment of a Turbulent Shear Layer," J. Fluid Mechanics, vol. 52, pp. 113-135.

Coles, D.F. "The Law of the Wall in Turbulent Shear Flow", **50 Jahre Grenzschichtforschung** (H. Goertler and W. Tollmien, eds.). F. Vieweg and Sohn, Braunschweig, pp. 153-163.

Hanson, C.E. (1969), "The Design and Construction of a Low Noise, Low Turbulence Wind Tunnel", Acoustics & Vibration Laboratory M.I.T. Report no. 79611-1.

Kline, S.J., Reynolds, W.C., Schraub, F.A., "The Structure of Turbulent Boundary Layers", J. Fluid Mechanics, vol. 30, part 4, pp. 741-773.

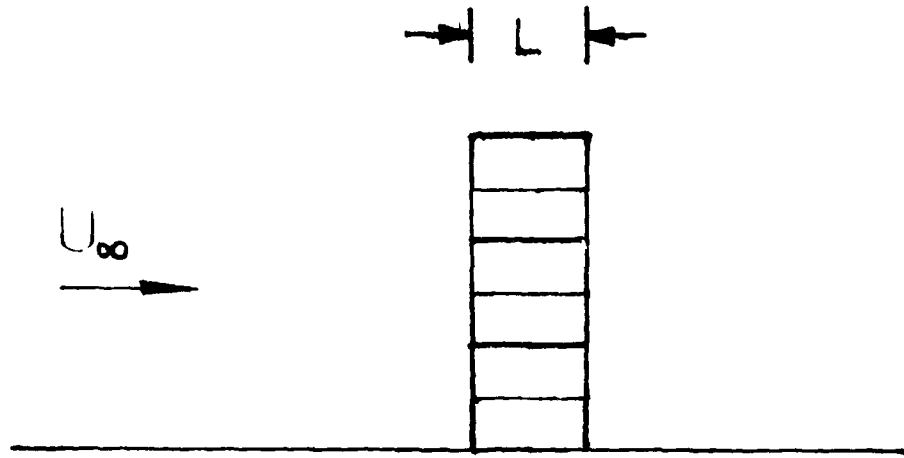
Moller, James Christian and Patrick Leehey, "Measurement of Wall Shear and Pressure Downstream of a Honeycomb Boundary Layer Manipulator." M.I.T. Acoustics and Vibration Laboratory Report no. 97457-3, April, 1989.

Potter, Merle C. and Foss, John F., **Fluid Mechanics**.  
(Great Lakes Press, Inc.: Okemos, MI , 1986).

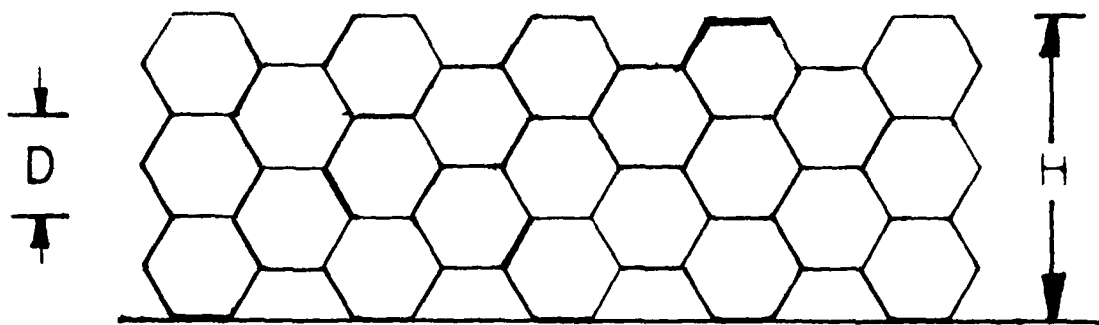
Savill, A.M. (1987), "On the Manner in Which Outer Layer Disturbances Affect Turbulent Boundary Layer Skin Friction," Advances in Turbulence; Proceedings of the First European Turbulence Conference, Ecully, France, July 1-4, 1986 (A87-52001 23-34). Berlin and New York, Springer-Verlag, pp. 533-545.

Schlichting, H., **Boundary Layer Theory, Seventh Edition**.  
(McGraw-Hill: New York, New York, 1979).

Shapiro, Paul J., "The Influence of Sound Upon Laminar Boundary Layer Instability", M.I.T. Acoustics & Vibration Laboratory Report no. 83458-83560-1, Sept., 1977.



Side View



Front View

Figure 1: Diagram of Honeycomb LEBU

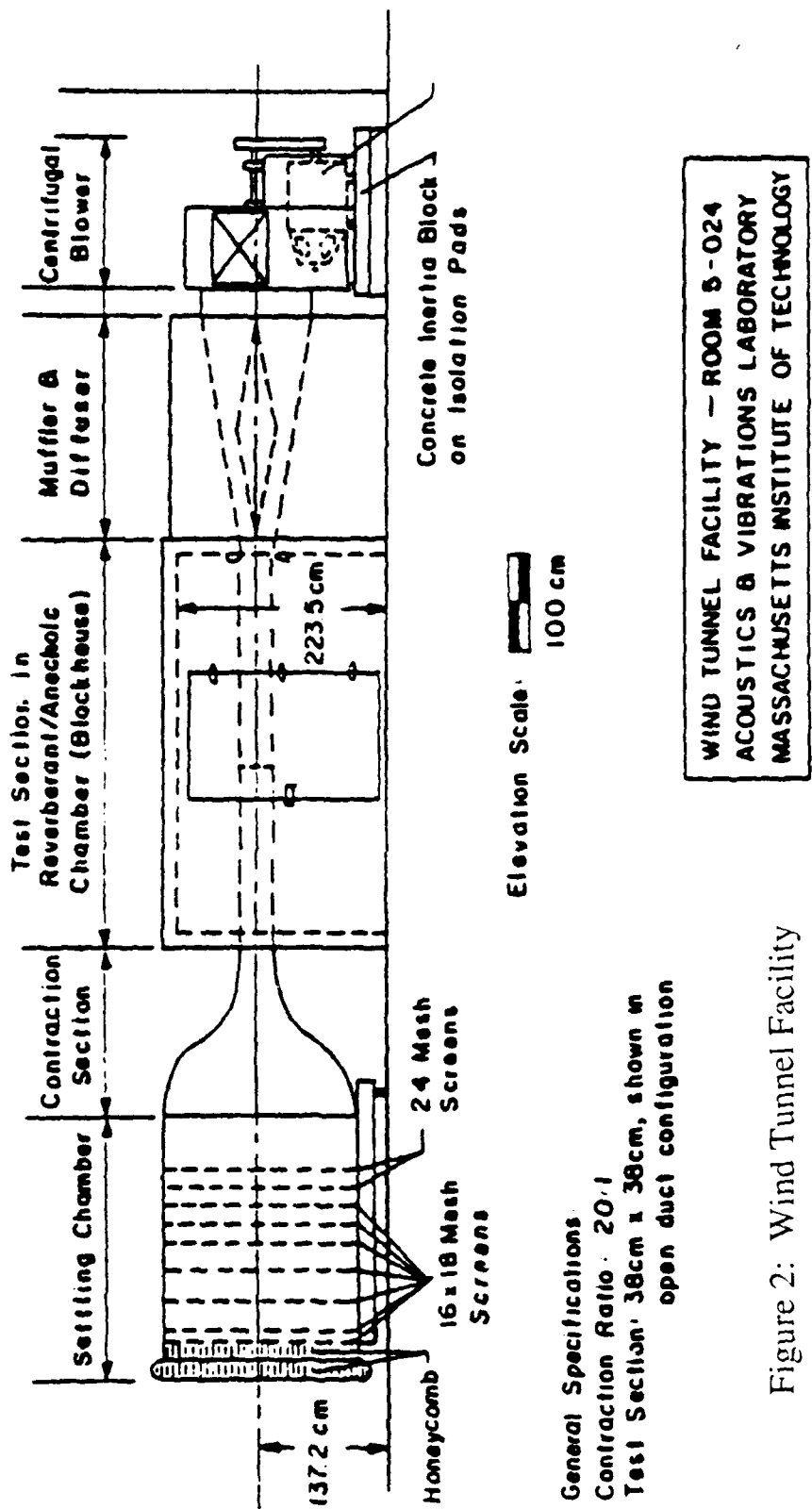


Figure 2: Wind Tunnel Facility



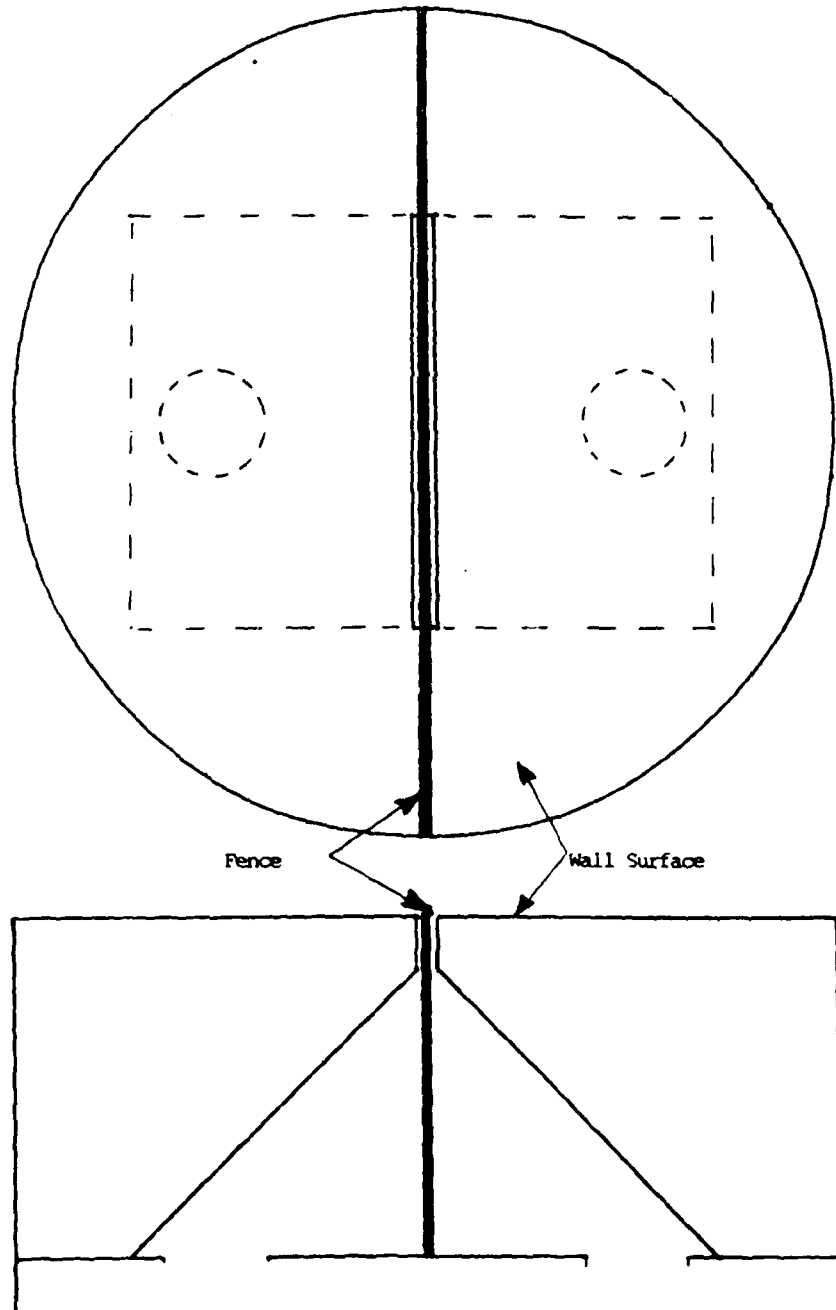


Figure 3: Diagram of Sublayer Surface Fence.

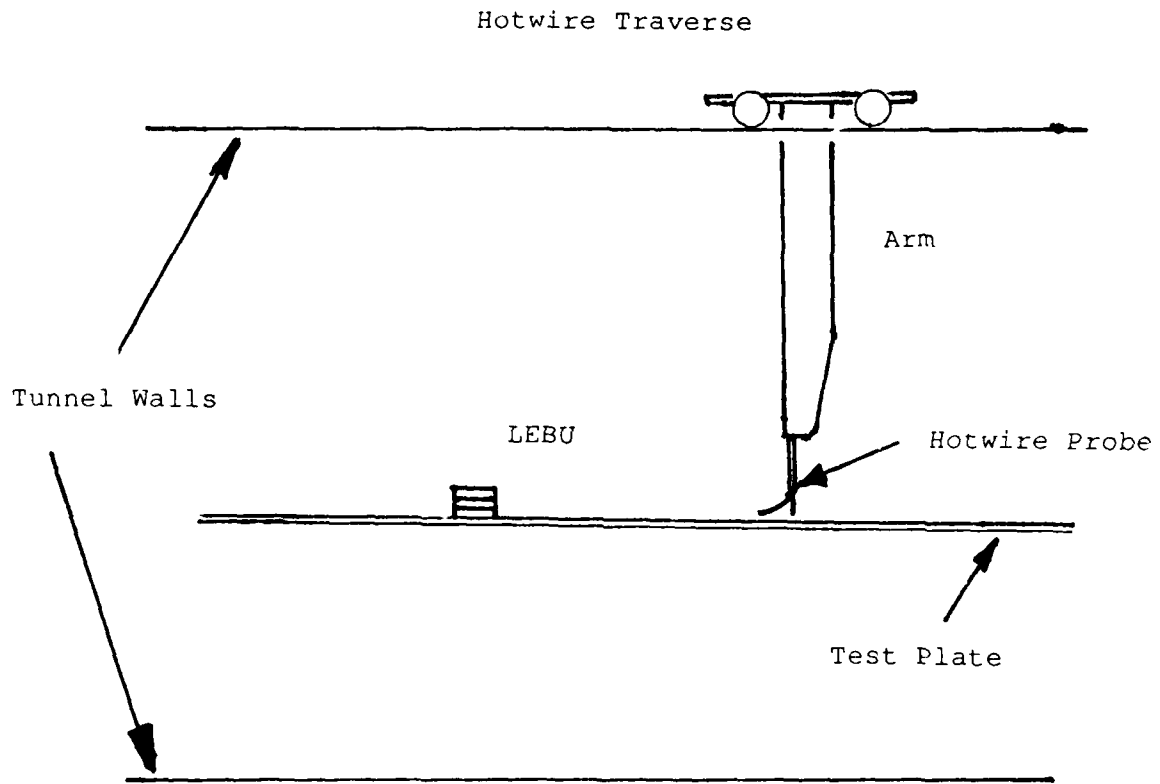


Figure 4: Hotwire Traverse

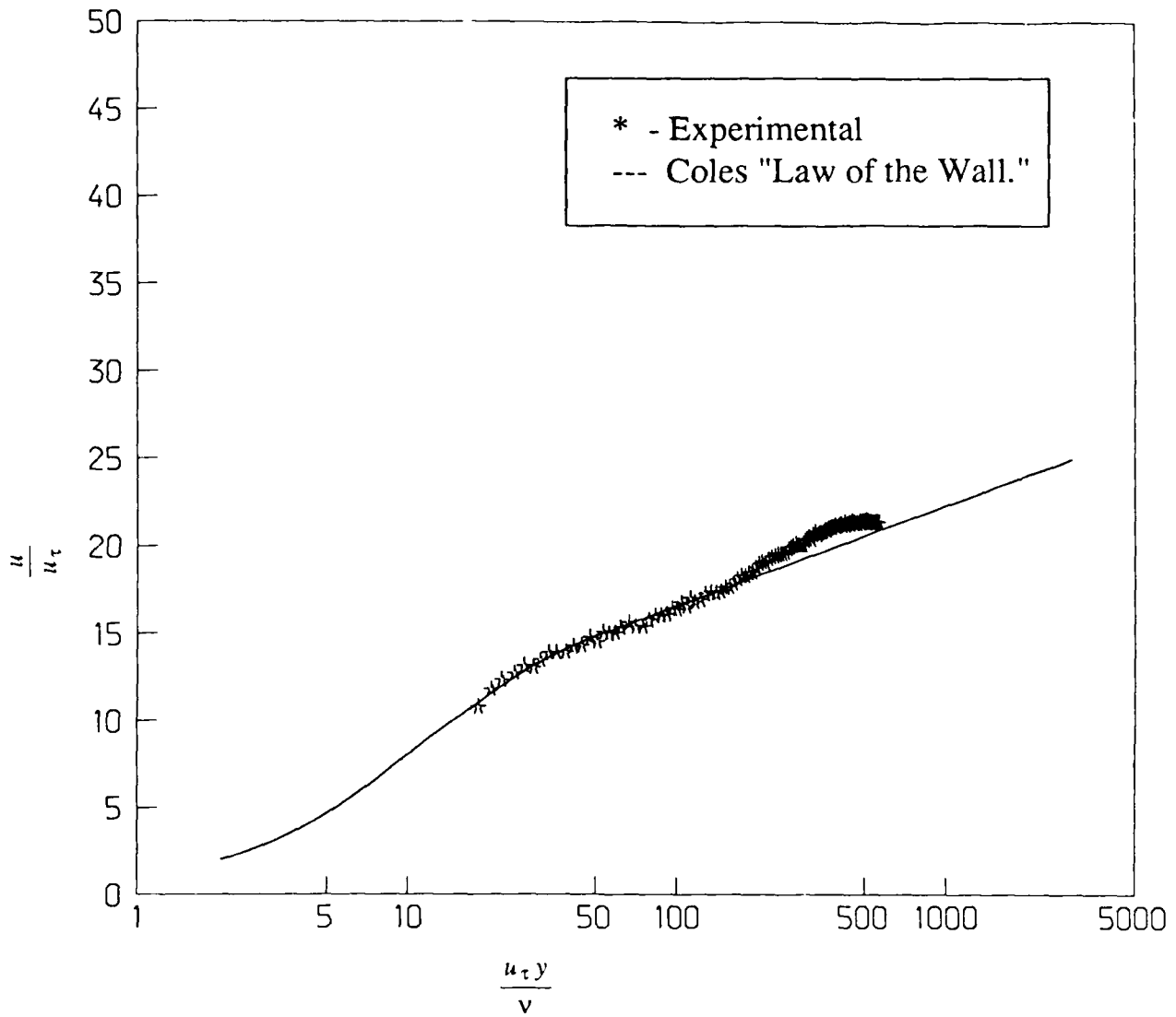


Figure 5a.: Unmanipulated Coles "Law of the Wall" Plot,  
 $U_\infty = 5 \text{ m/s}$ ,  $x_{LEBU} = 16.5 \text{ in}$ .

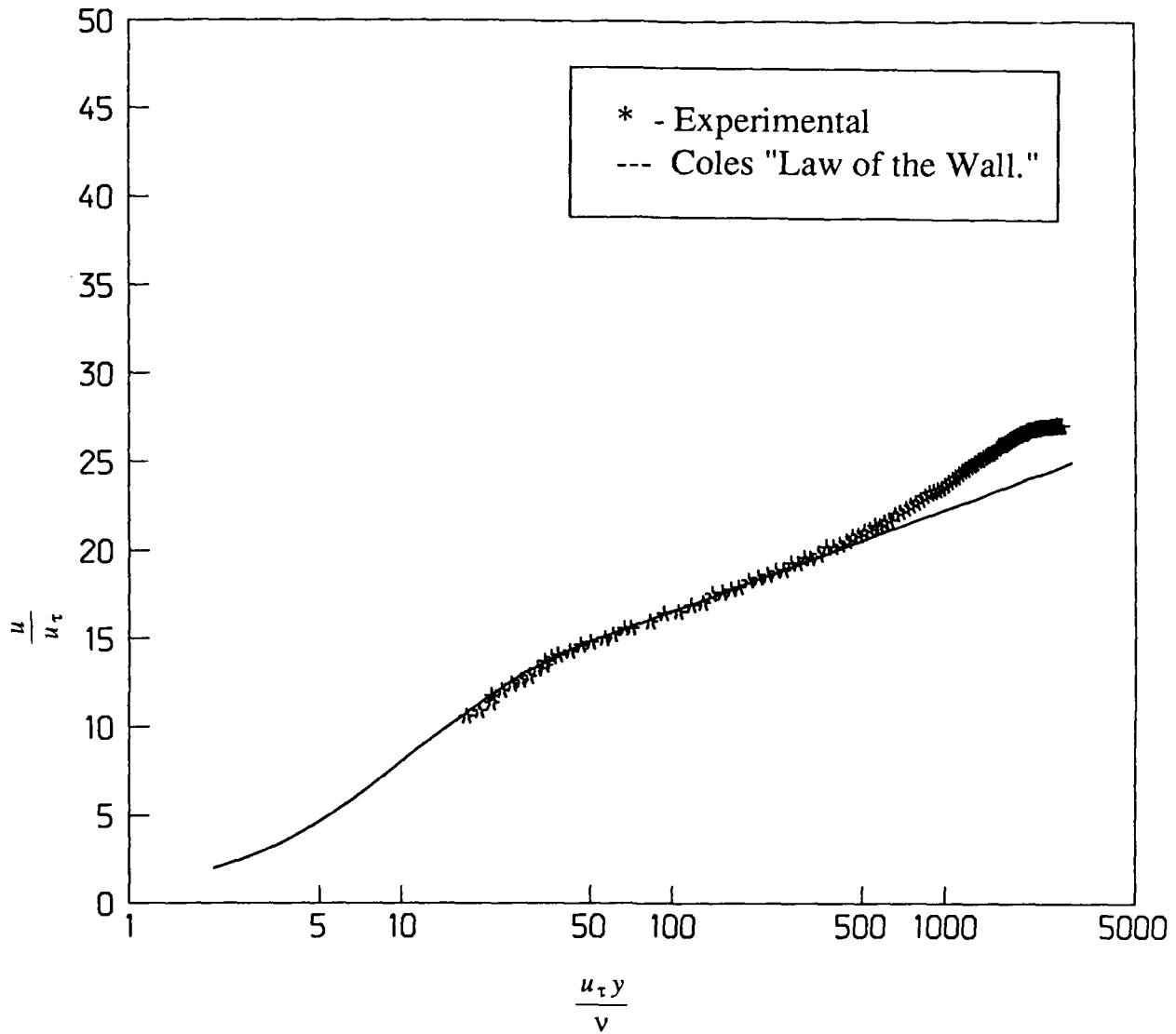


Figure 5b.: Unmanipulated Coles "Law of the Wall" Plot,  
 $U_\infty = 35 \text{ m/s}$ ,  $x_{LEBU} = 16.5 \text{ in.}$

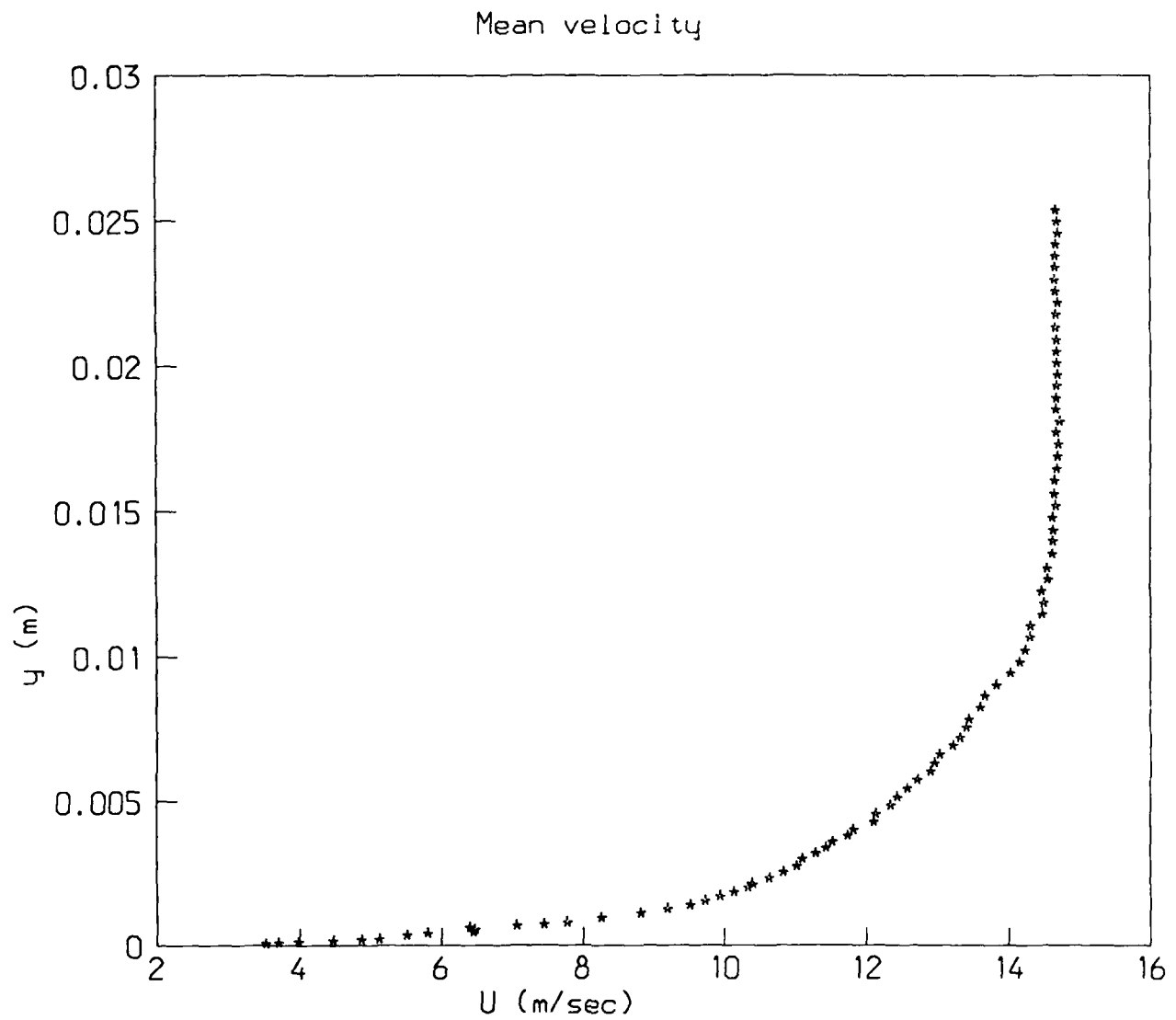


Figure 6a.: Unmanipulated Mean Velocity Profile,  
 $x_{LEBU} = 0 \text{ in.}$ ,  $U_{\infty} = 15 \text{ m/s.}$

Mean velocity

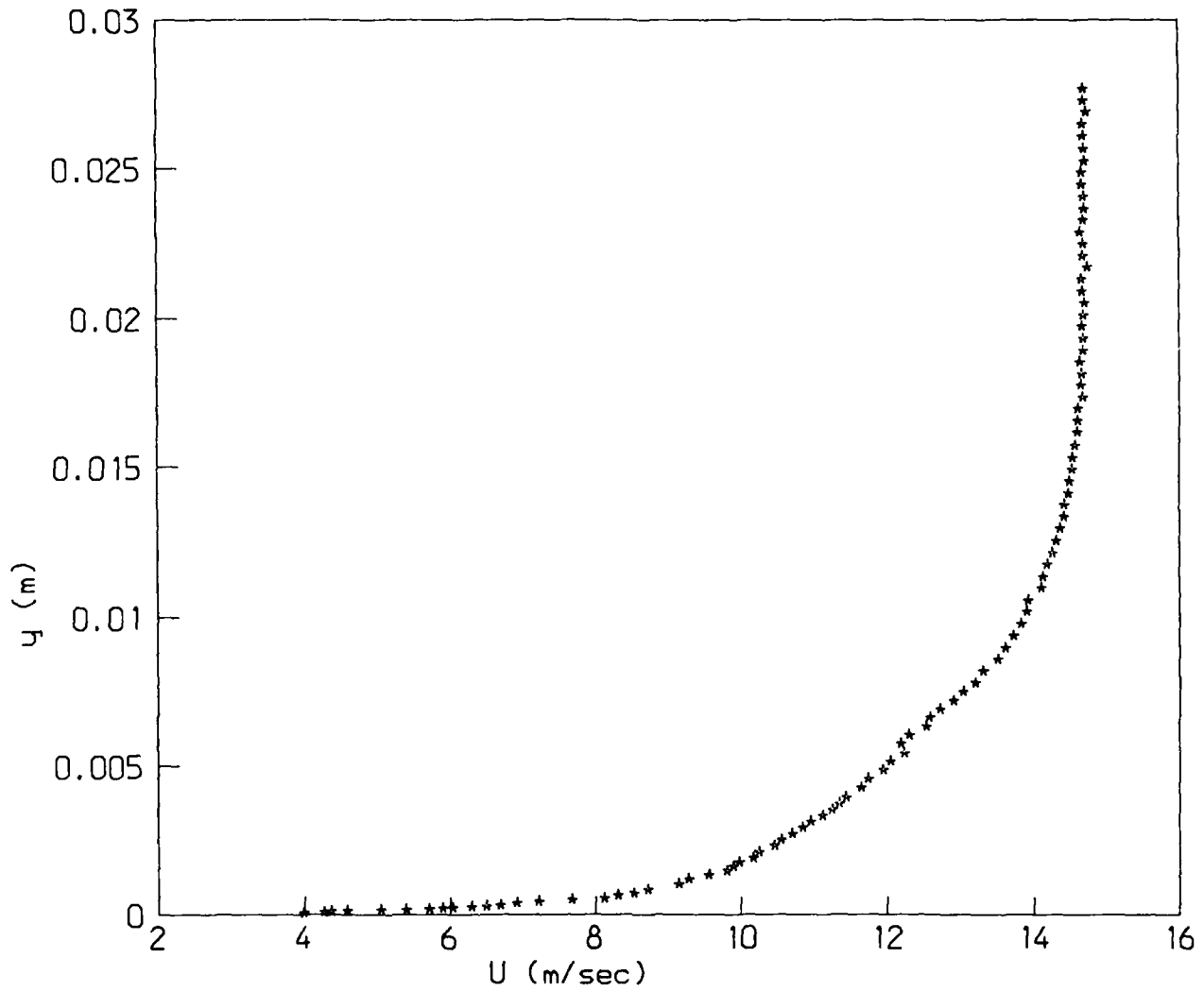


Figure 6b.: Unmanipulated Mean Velocity Profile,  
 $x_{LEBU} = 5in. , U_{\infty} = 15 m/s .$

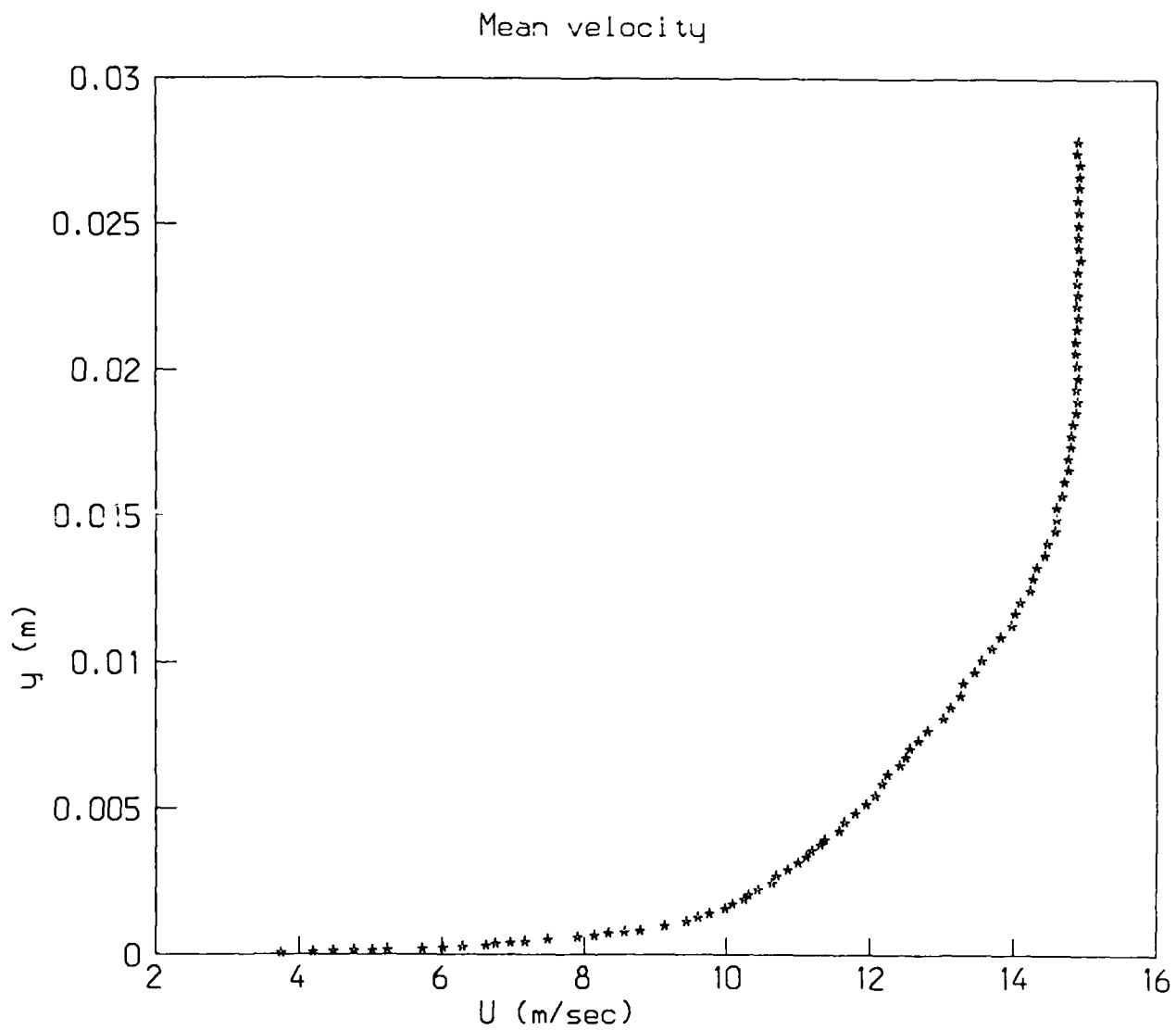


Figure 6c.: Unmanipulated Mean Velocity Profile,  
 $x_{LEBU} = 10in.$ ,  $U_{\infty} = 15 m/s.$

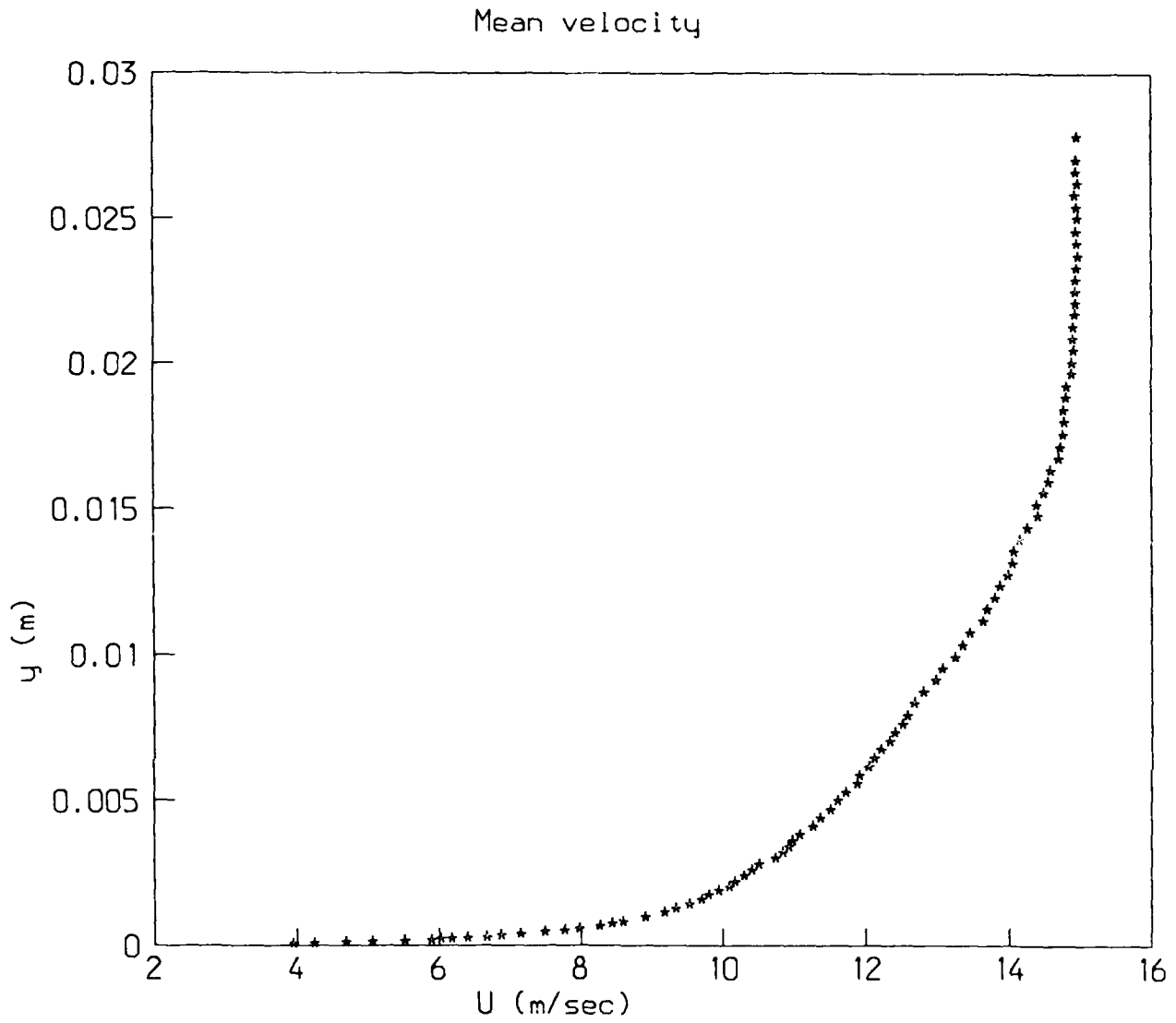


Figure 6d.: Unmanipulated Mean Velocity Profile,  
 $x_{LEBU} = 15in.$ ,  $U_{\infty} = 15 m/s.$



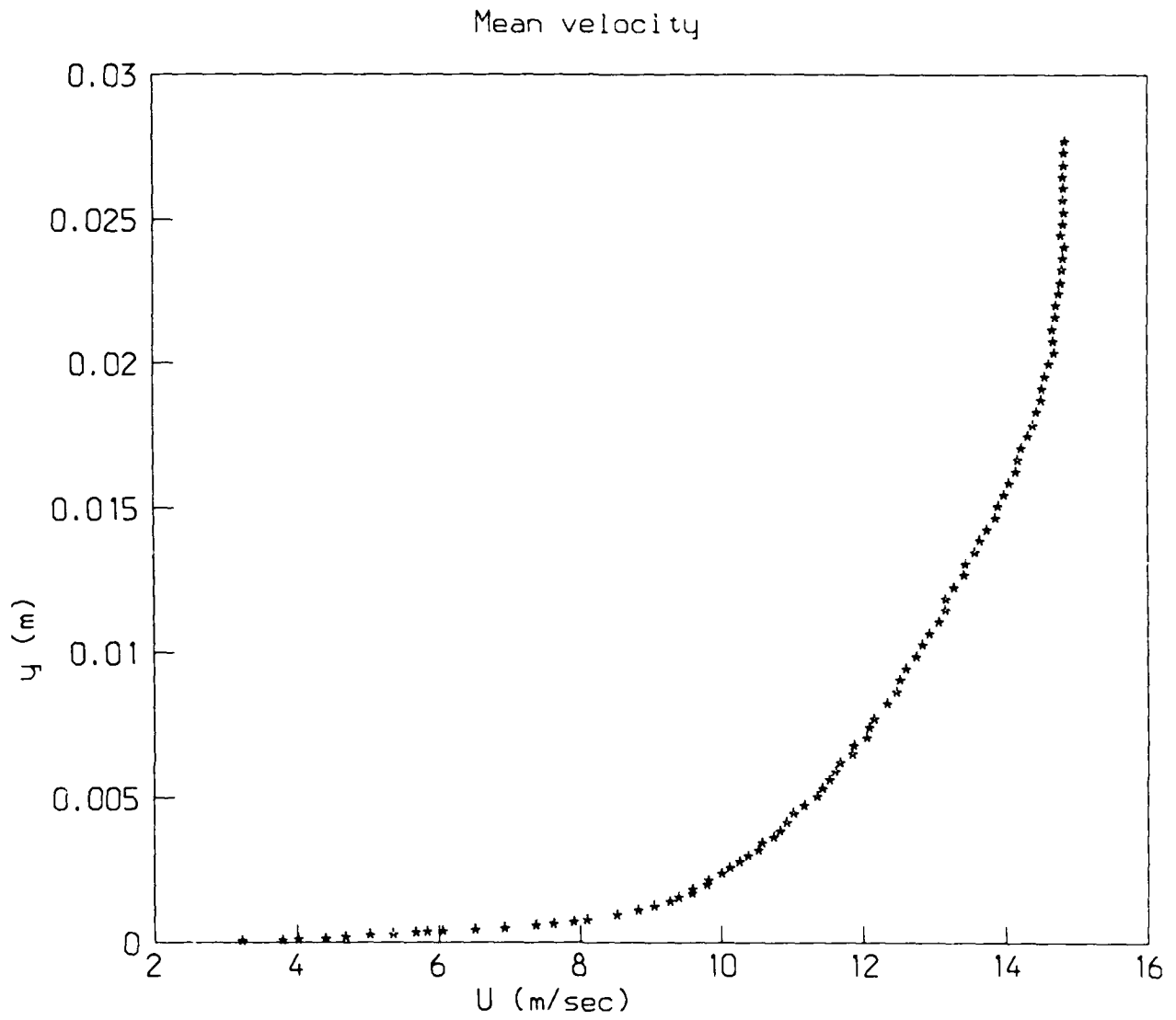


Figure 6e.: Unmanipulated Mean Velocity Profile,  
 $x_{LEBU} = 20in.$ ,  $U_{\infty} = 15 m/s.$

Mean velocity

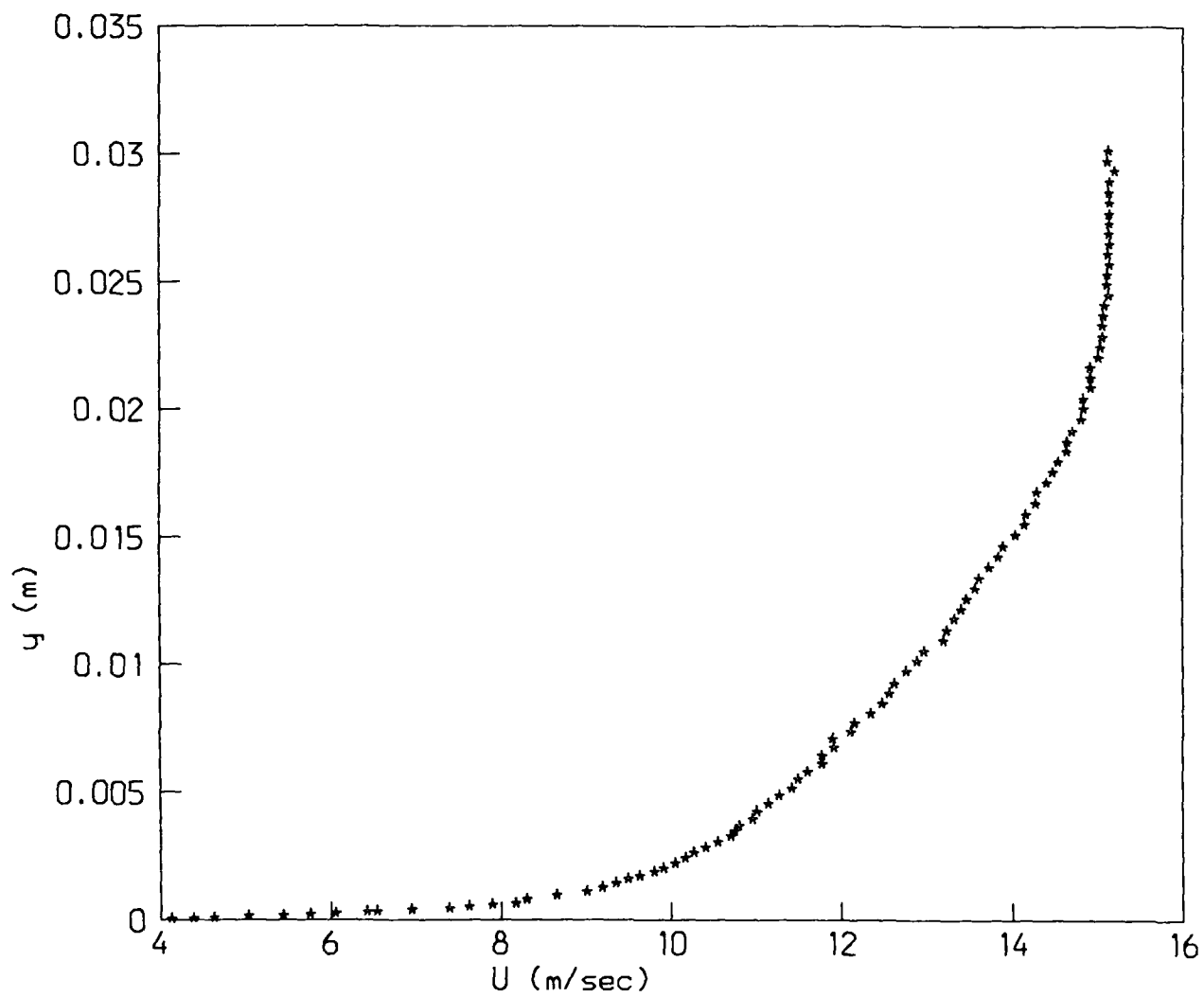


Figure 6f.: Unmanipulated Mean Velocity Profile,  
 $x_{LEBU} = 25in.$ ,  $U_{\infty} = 15 m/s.$

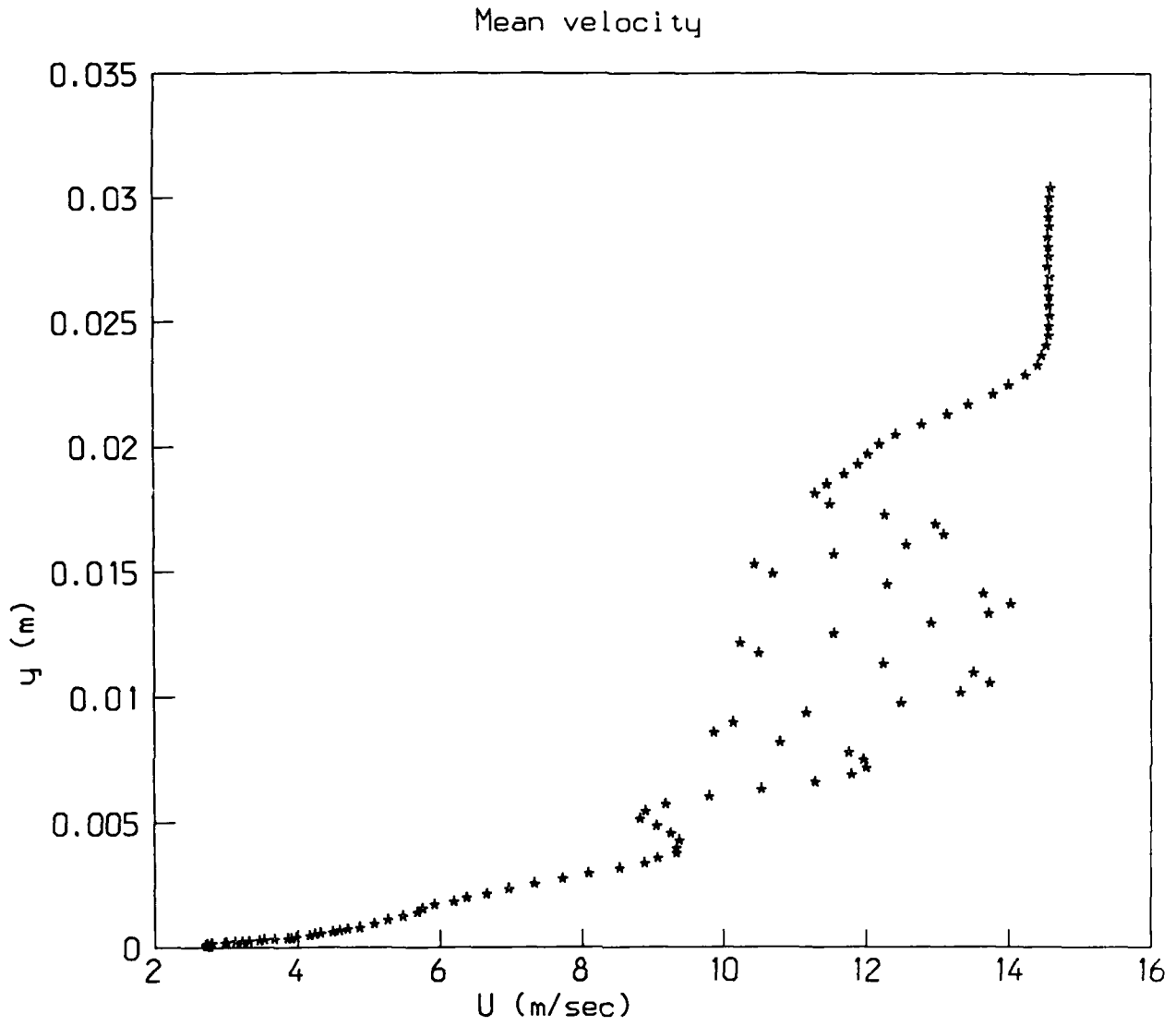


Figure 7a.: Manipulated Mean Velocity Profile, 6 - 1/8" cells LEBU,  
 $x_{LEBU} = 1in.$ ,  $U_{\infty} = 14 m/s.$

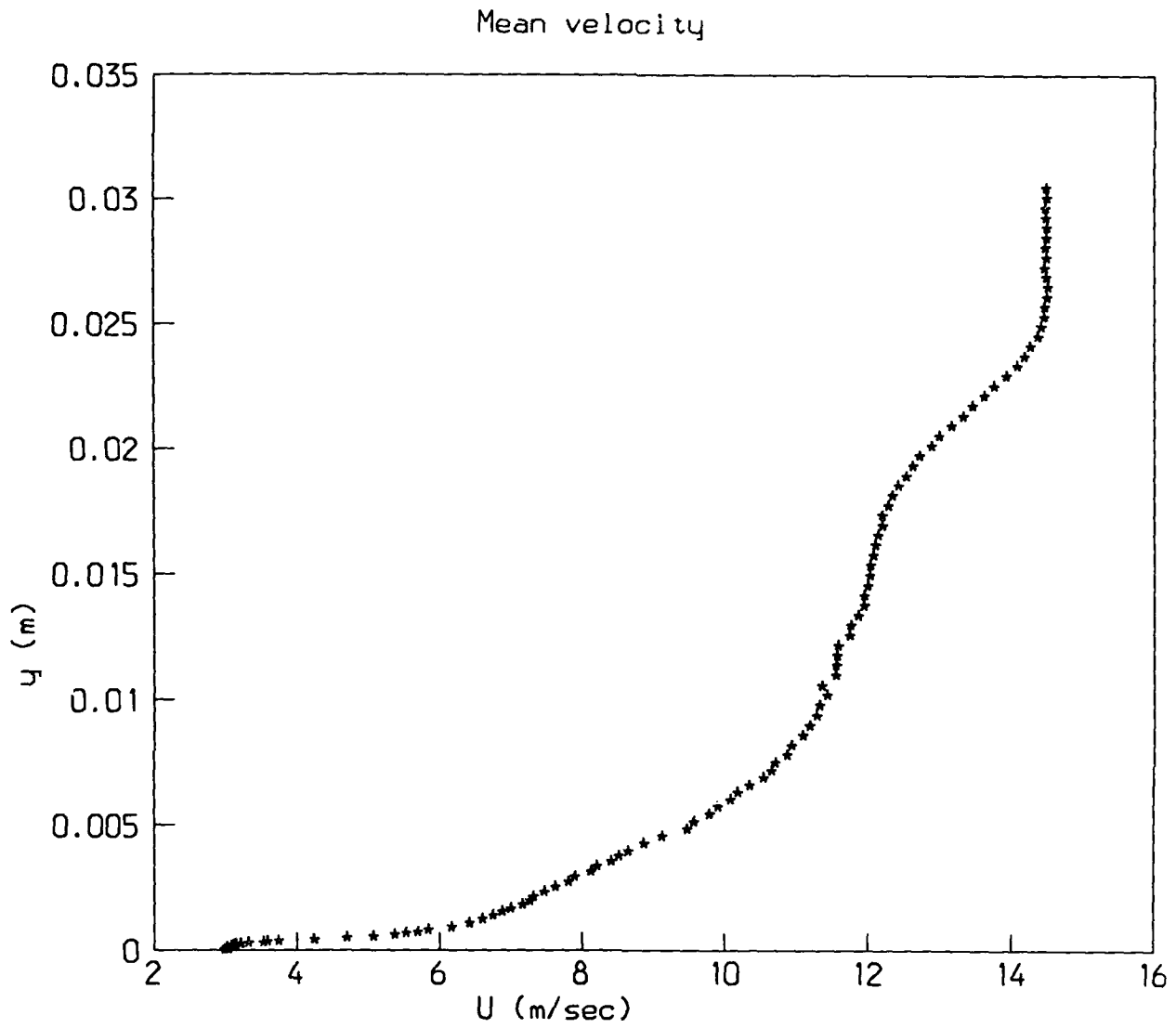


Figure 7b.: Manipulated Mean Velocity Profile, 6 - 1/8" cells LEBU,  
 $x_{LEBU} = 3in.$ ,  $U_{\infty} = 14 m/s.$

Mean velocity

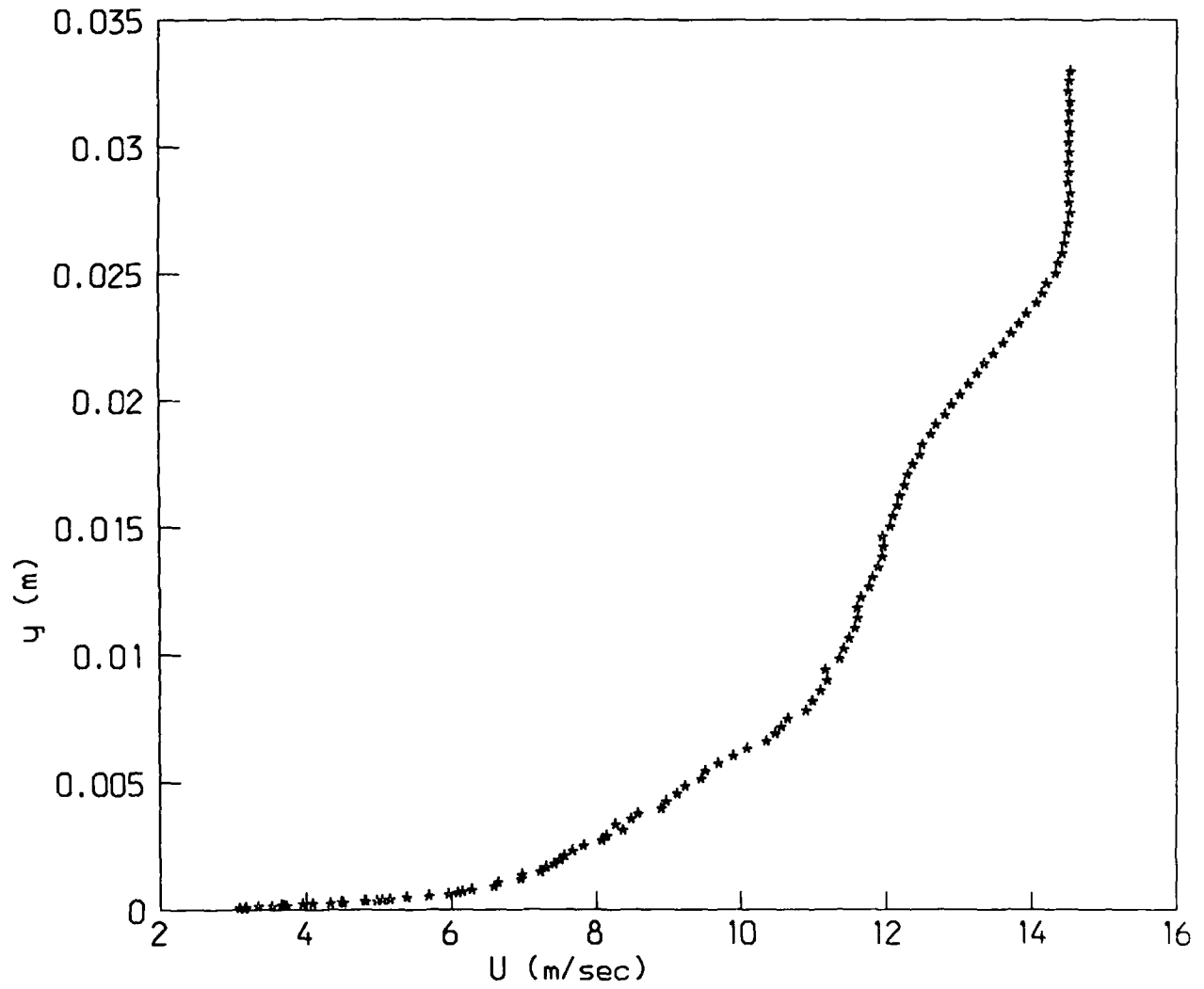


Figure 7c.: Manipulated Mean Velocity Profile, 6 - 1/8" cells LEBU,  
 $x_{LEBU} = 5in.$ ,  $U_{\infty} = 14 m/s.$

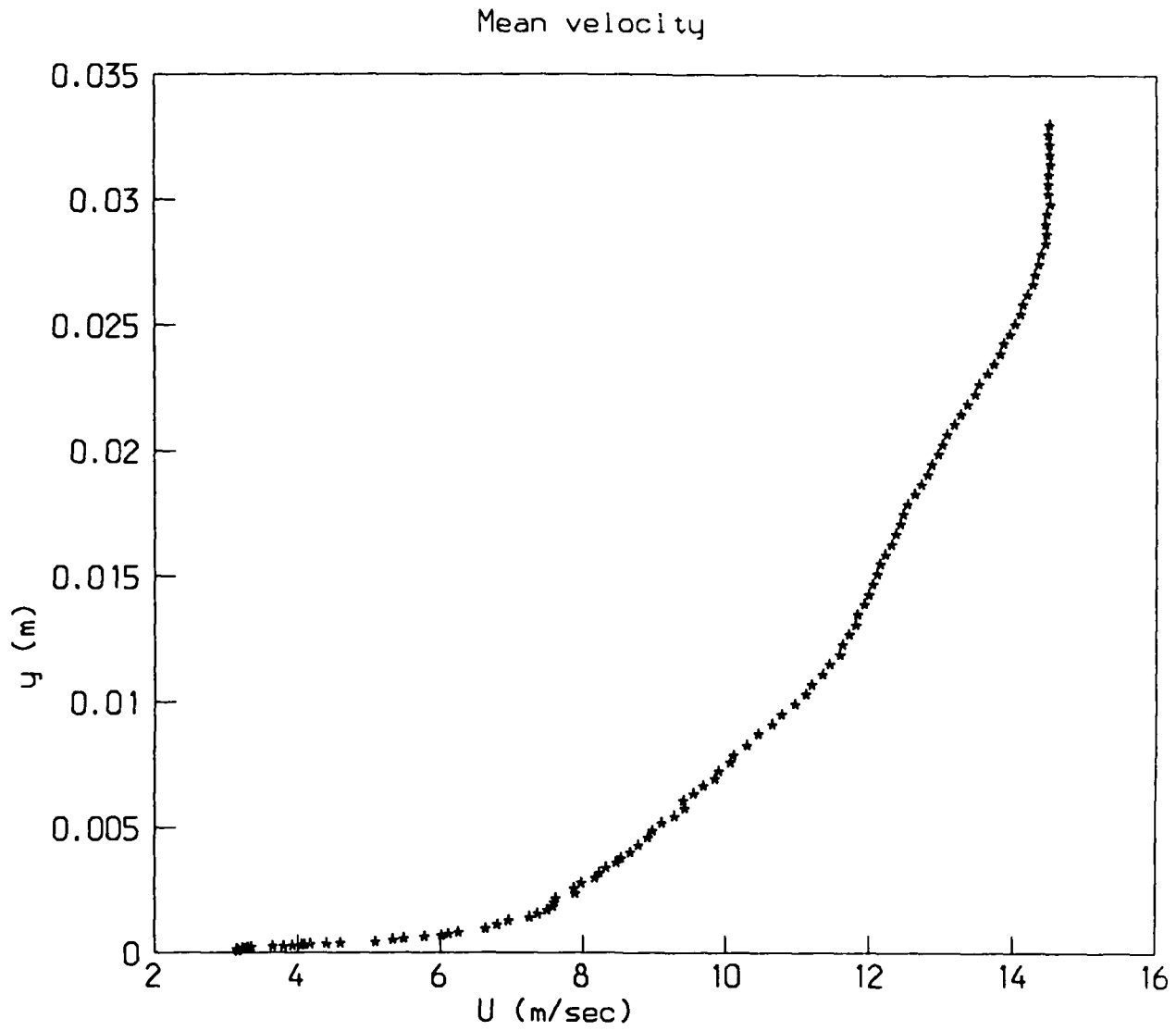


Figure 7d.: Manipulated Mean Velocity Profile, 6 - 1/8" cells LEBU,  
 $x_{LEBU} = 10in.$ ,  $U_{\infty} = 14 m/s.$

Mean velocity

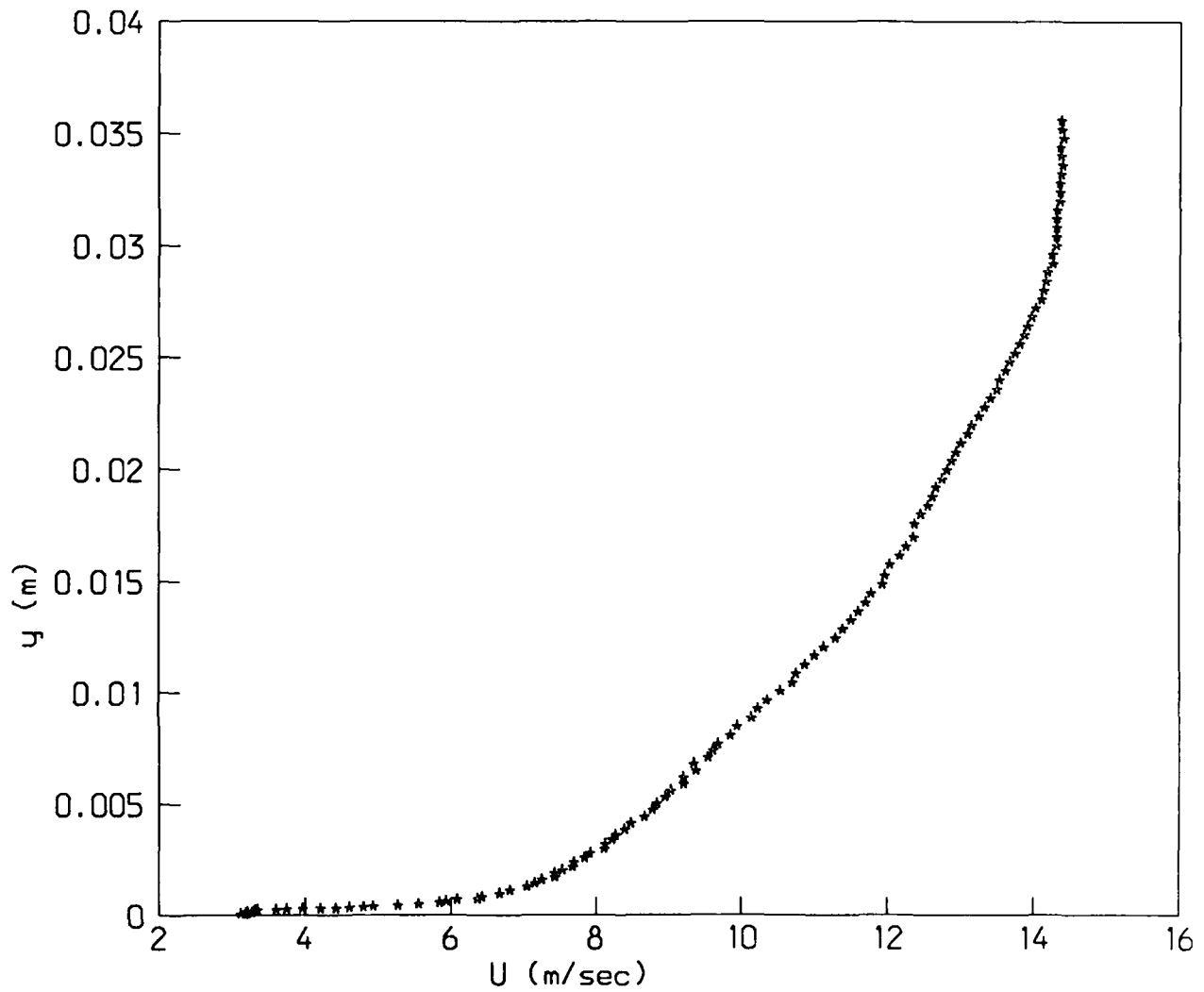


Figure 7e.: Manipulated Mean Velocity Profile, 6 - 1/8" cells LEBU,  
 $x_{LEBU} = 15in.$ ,  $U_{\infty} = 14 m/s.$

Mean velocity

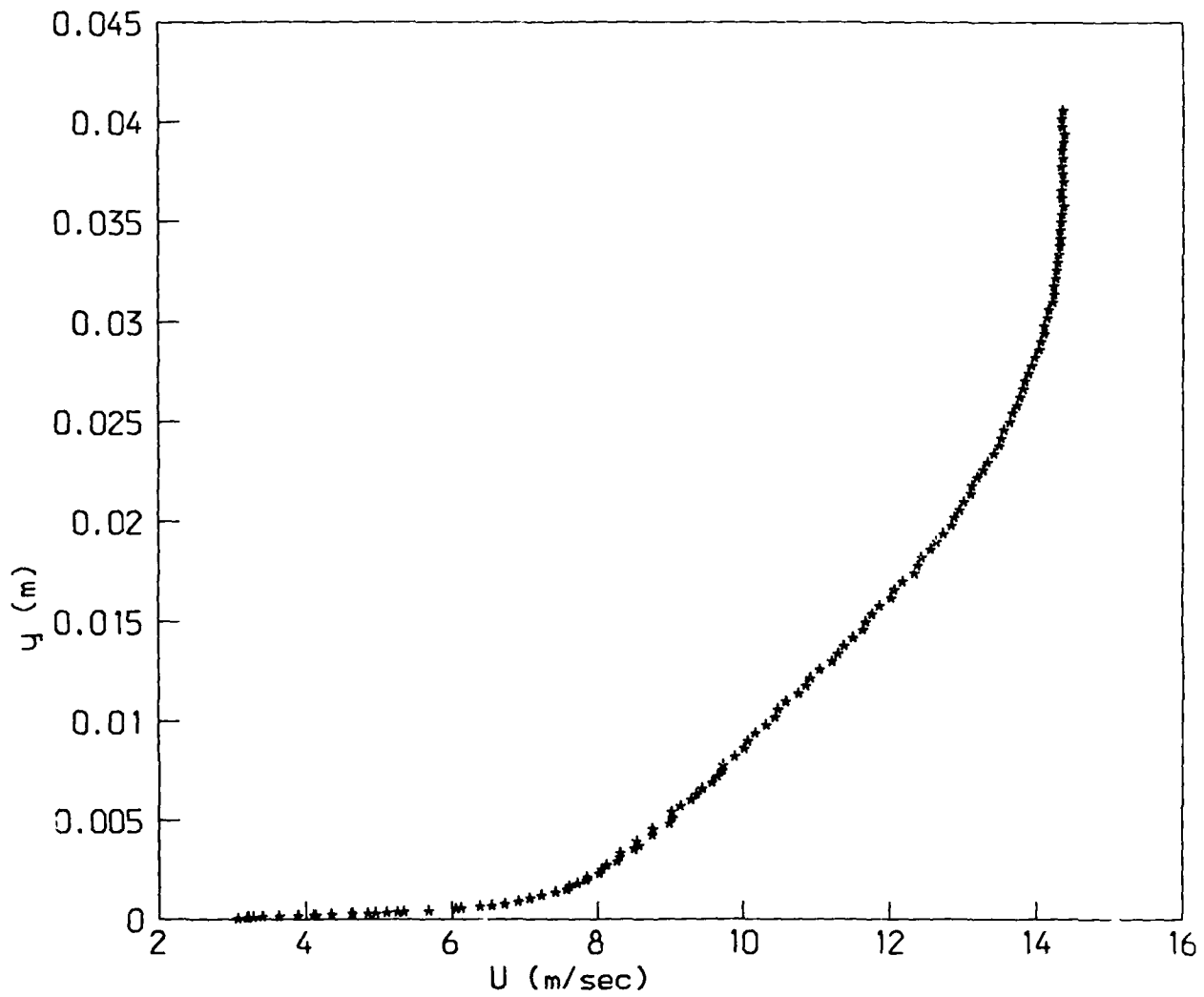


Figure 7f.: Manipulated Mean Velocity Profile, 6 - 1/8" cells LEBU,  
 $x_{LEBU} = 25in.$ ,  $U_{\infty} = 14 m/s.$



Mean velocity

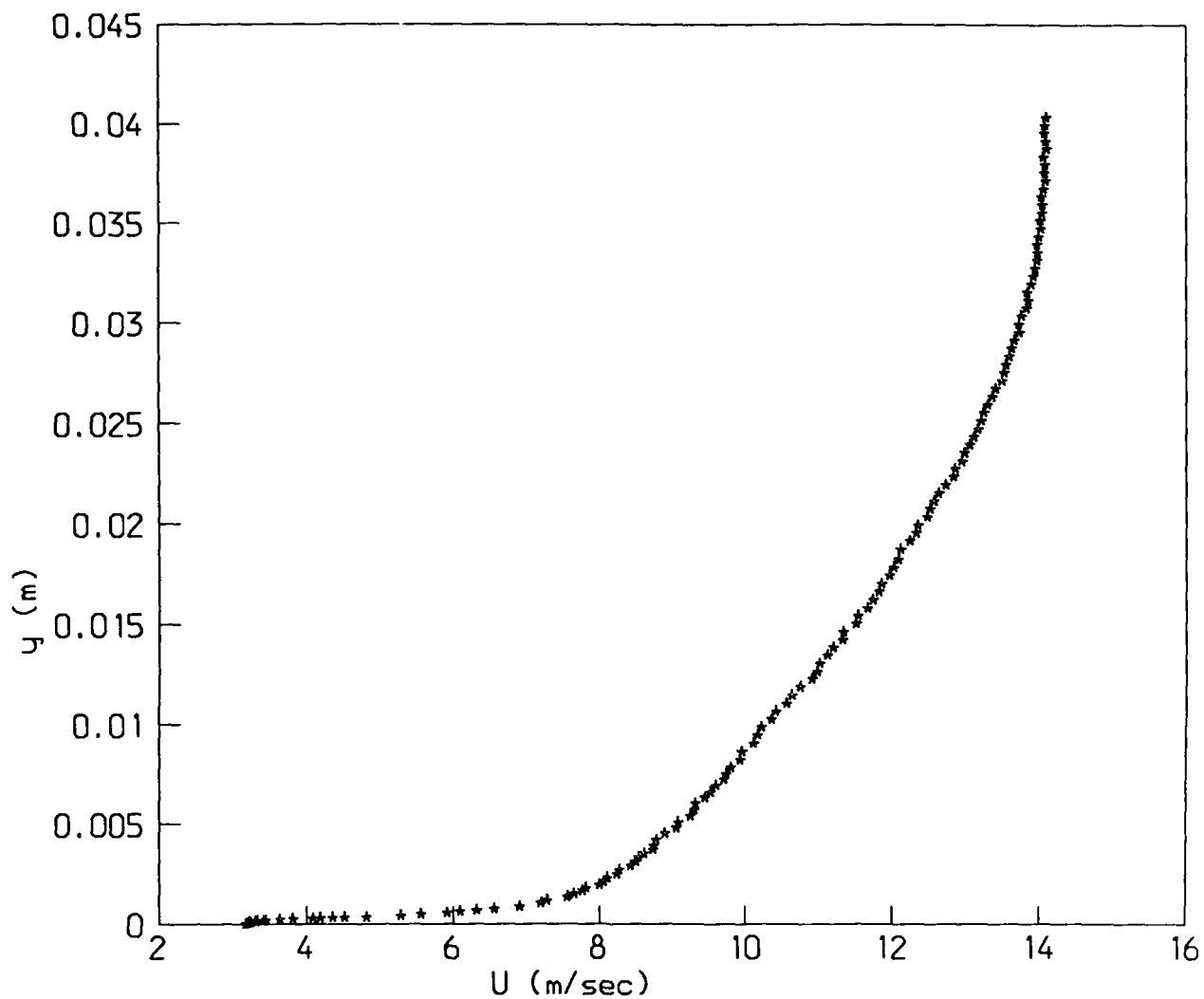


Figure 7g.: Manipulated Mean Velocity Profile, 6 - 1/8" cells LEBU,  
 $x_{LEBU} = 35in.$ ,  $U_{\infty} = 14 m/s$ .

Fluctuating velocity

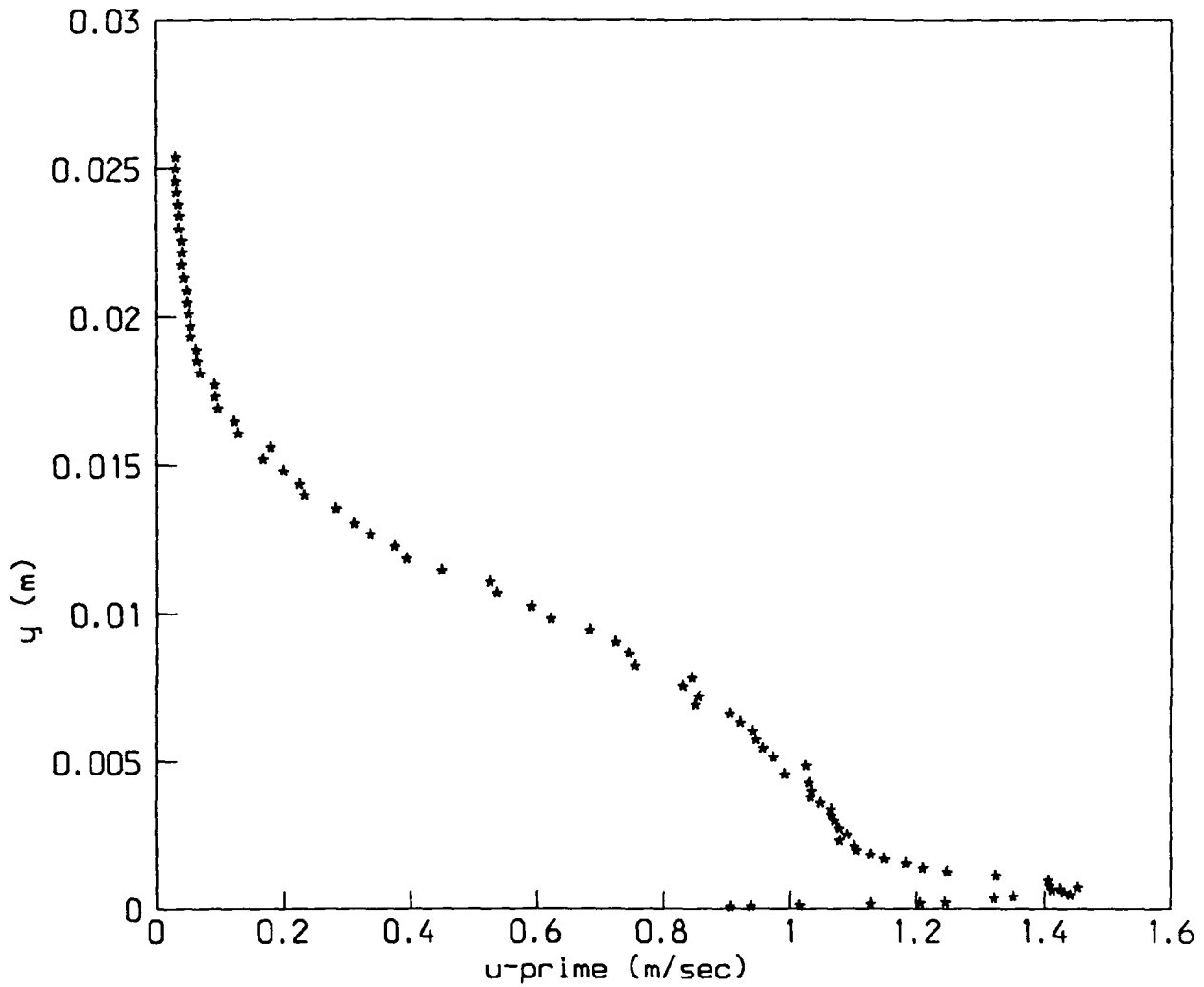


Figure 8a.: Unmanipulated Fluctuating Velocity Profile,  
 $x_{LEBU} = 0 \text{ in.}$ ,  $U_{\infty} = 15 \text{ m/s.}$

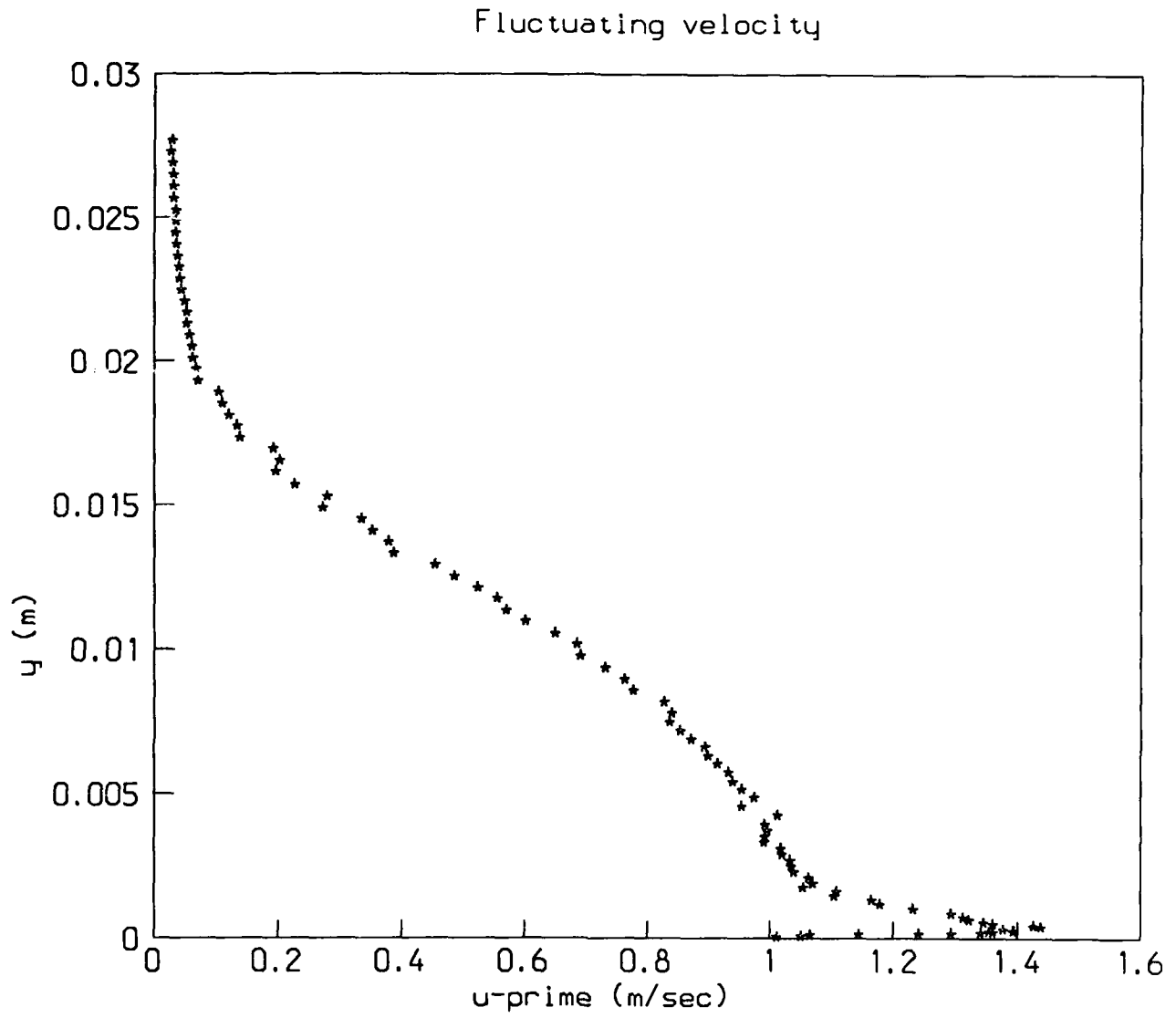


Figure 8b.: Unmanipulated Fluctuating Velocity Profile,  
 $x_{LEBU} = 5in. , U_{\infty} = 15 m/s .$

Fluctuating velocity

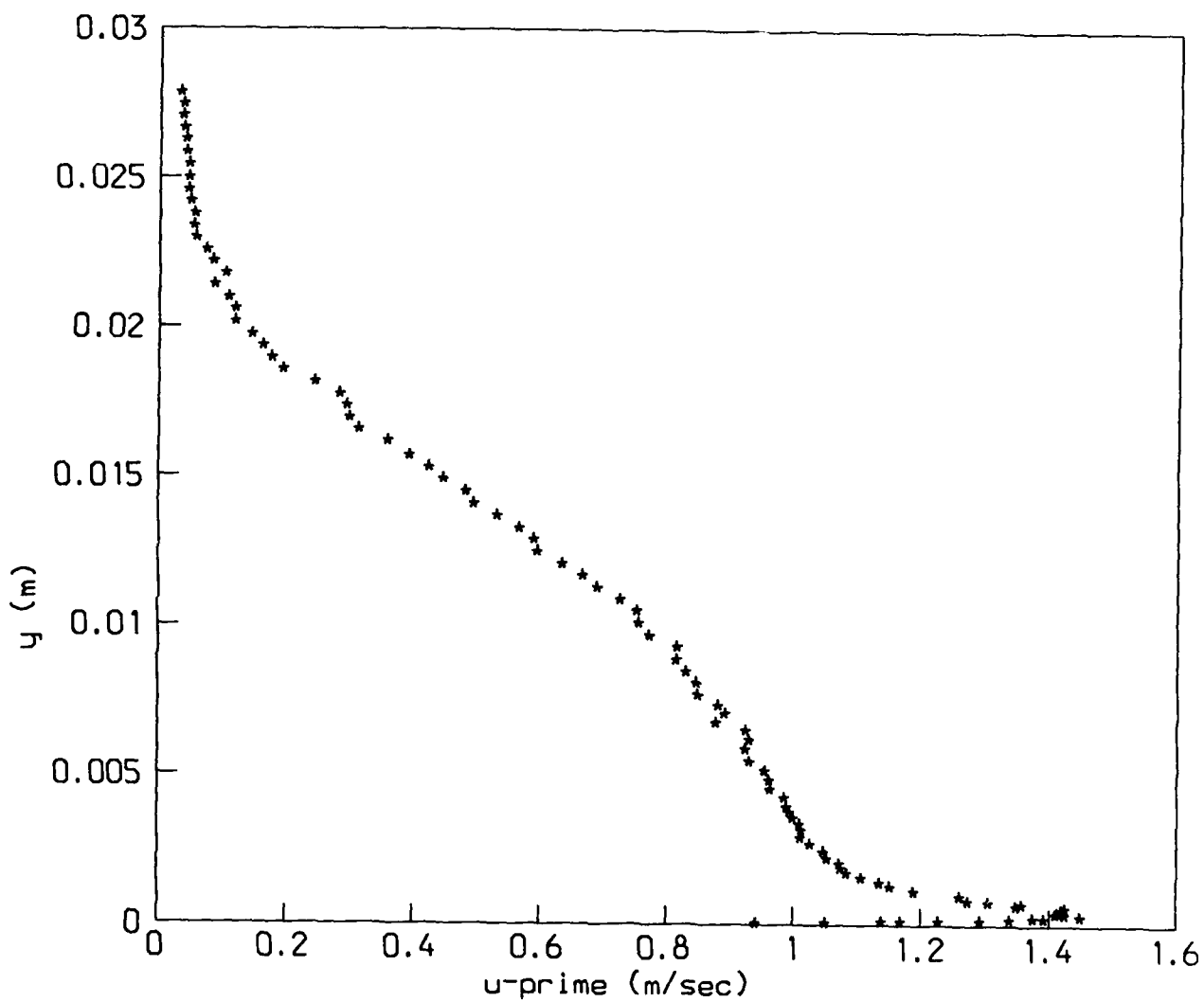


Figure 8c.: Unmanipulated Fluctuating Velocity Profile,  
 $x_{LEBU} = 10in.$ ,  $U_{\infty} = 15 m/s.$

Fluctuating velocity

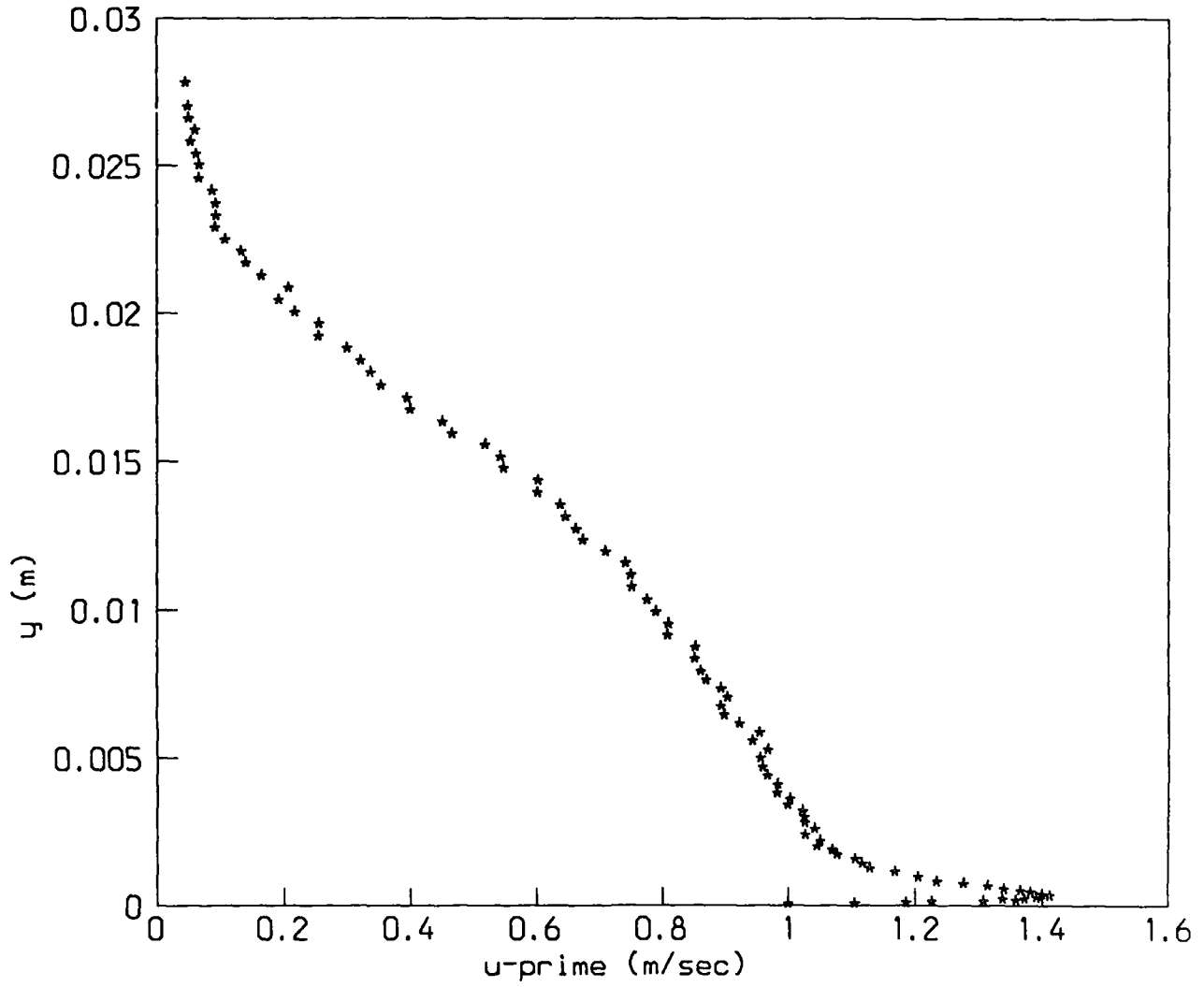


Figure 8d.: Unmanipulated Fluctuating Velocity Profile,  
 $x_{LEBU} = 15in.$ ,  $U_{\infty} = 15 m/s$ .

Fluctuating velocity

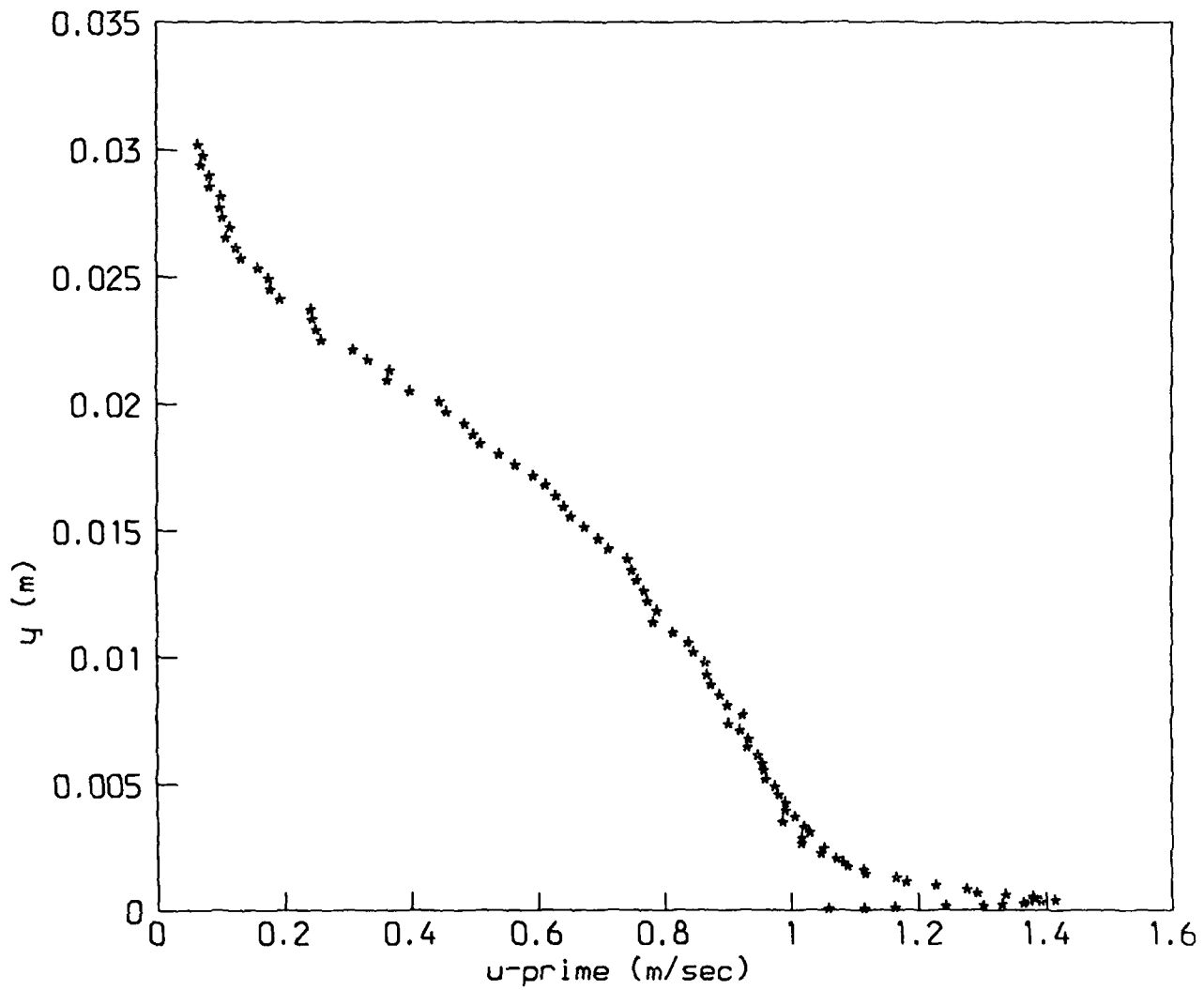


Figure 8e.: Unmanipulated Fluctuating Velocity Profile,  
 $x_{LEBU} = 25in.$ ,  $U_{\infty} = 15 m/s.$

Fluctuating velocity

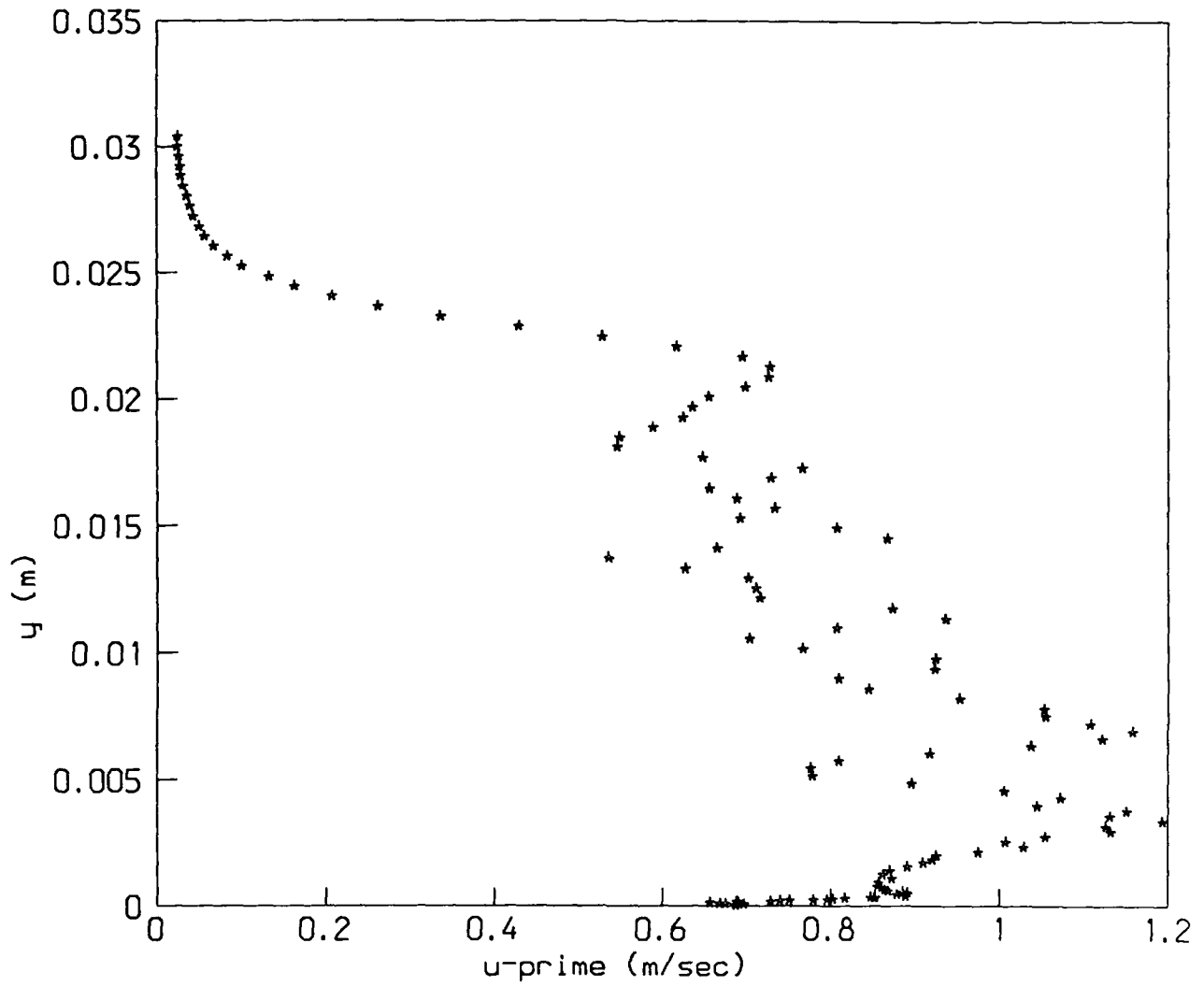


Figure 9a.: Manipulated Fluctuating Velocity Profile,  
6 - 1/8" cells LEBU,  $x_{LEBU} = 1in.$ ,  $U_{\infty} = 14 m/s.$

Fluctuating velocity

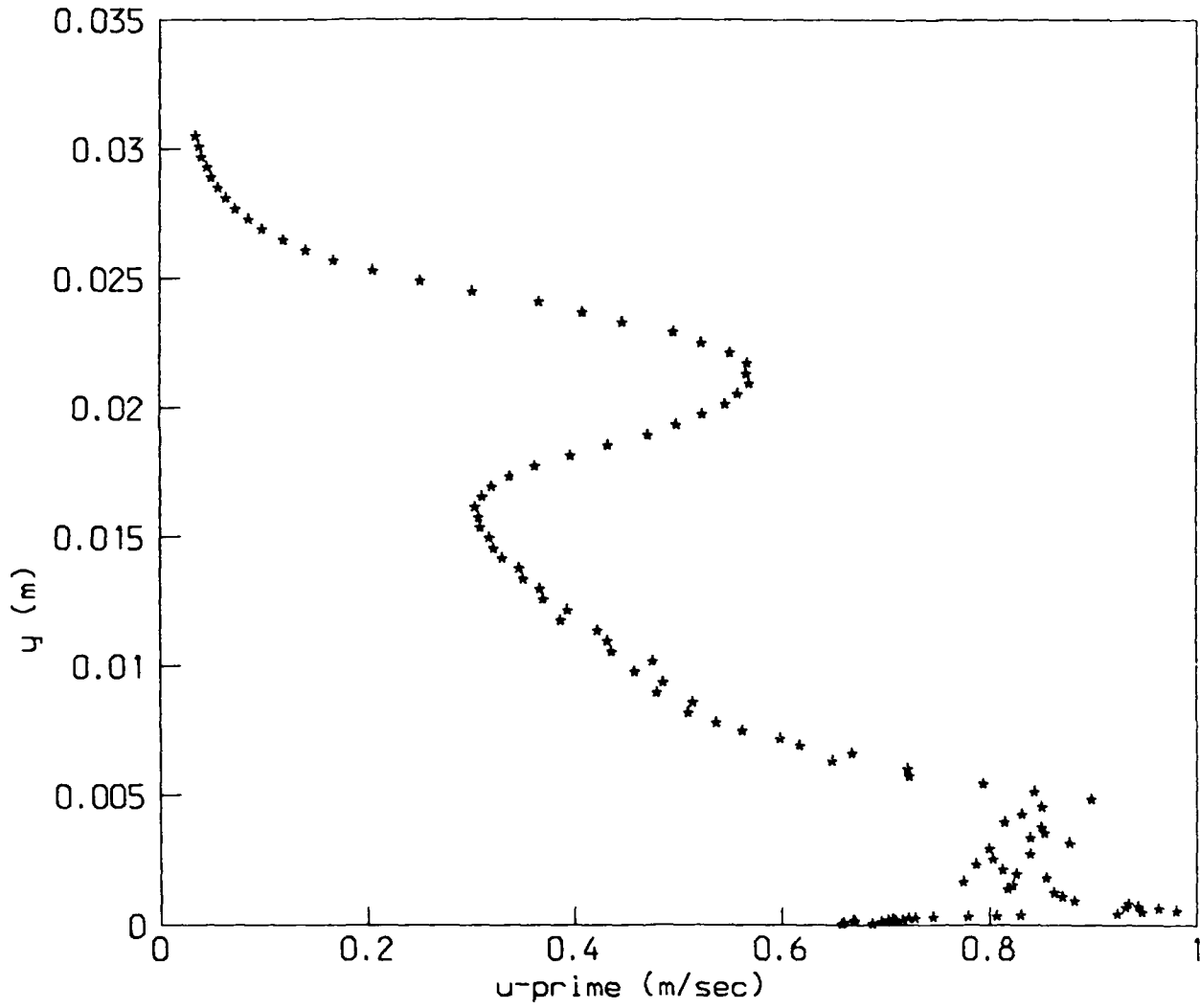


Figure 9b.: Manipulated Fluctuating Velocity Profile,  
6 - 1/8" cells LEBU,  $x_{LEBU} = 3in.$ ,  $U_{\infty} = 14 m/s$ .



Fluctuating velocity

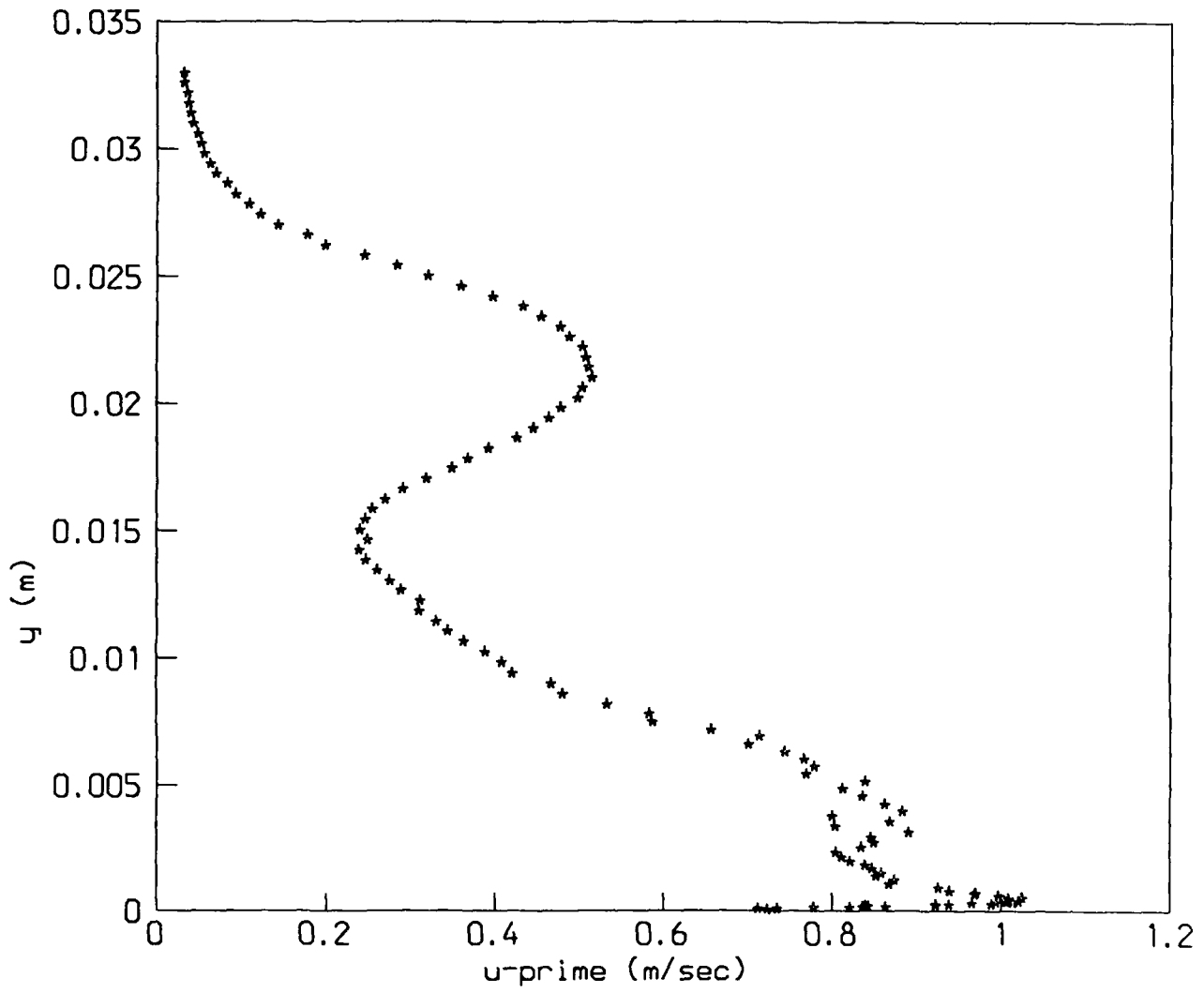


Figure 9c.: Manipulated Fluctuating Velocity Profile,  
6 - 1/8" cells LEBU,  $x_{LEBU} = 5in.$ ,  $U_{\infty} = 14 m/s.$

Fluctuating velocity

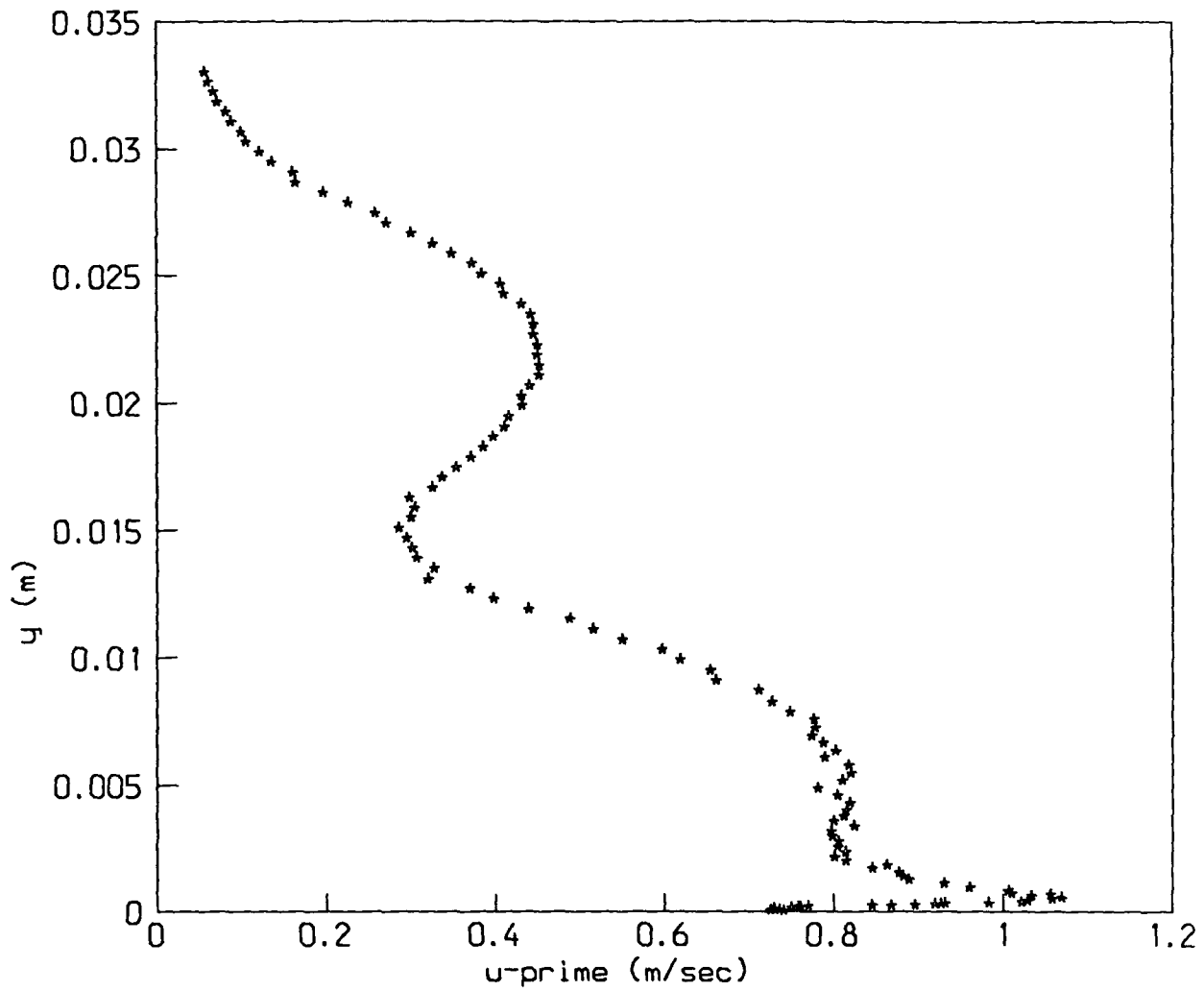


Figure 9d.: Manipulated Fluctuating Velocity Profile,  
6 - 1/8" cells LEBU,  $x_{LEBU} = 10in.$ ,  $U_{\infty} = 14 m/s.$

Fluctuating velocity

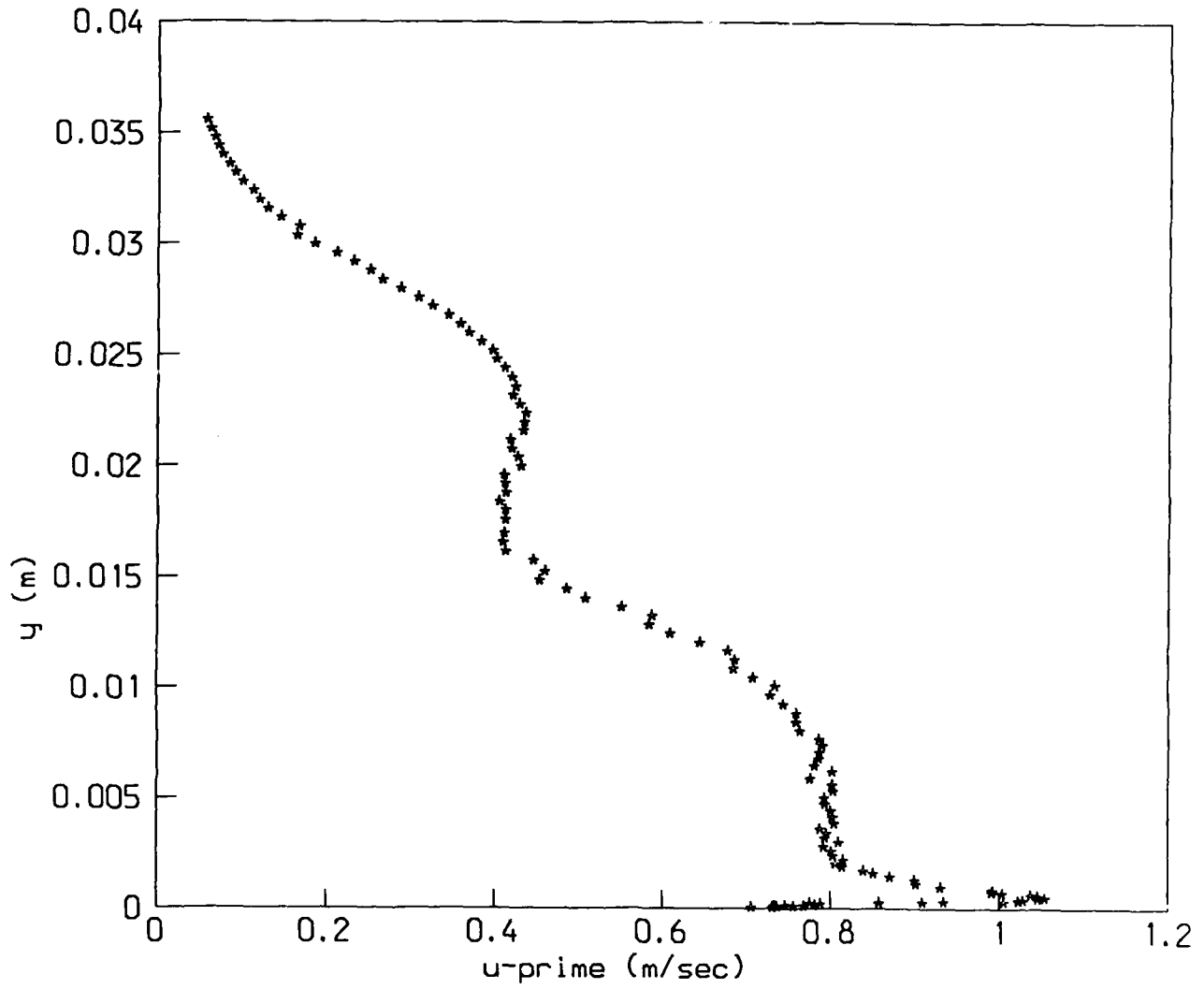


Figure 9e.: Manipulated Fluctuating Velocity Profile,  
6 - 1/8" cells LEBU,  $x_{LEBU} = 15in.$ ,  $U_{\infty} = 14 m/s.$

Fluctuating velocity

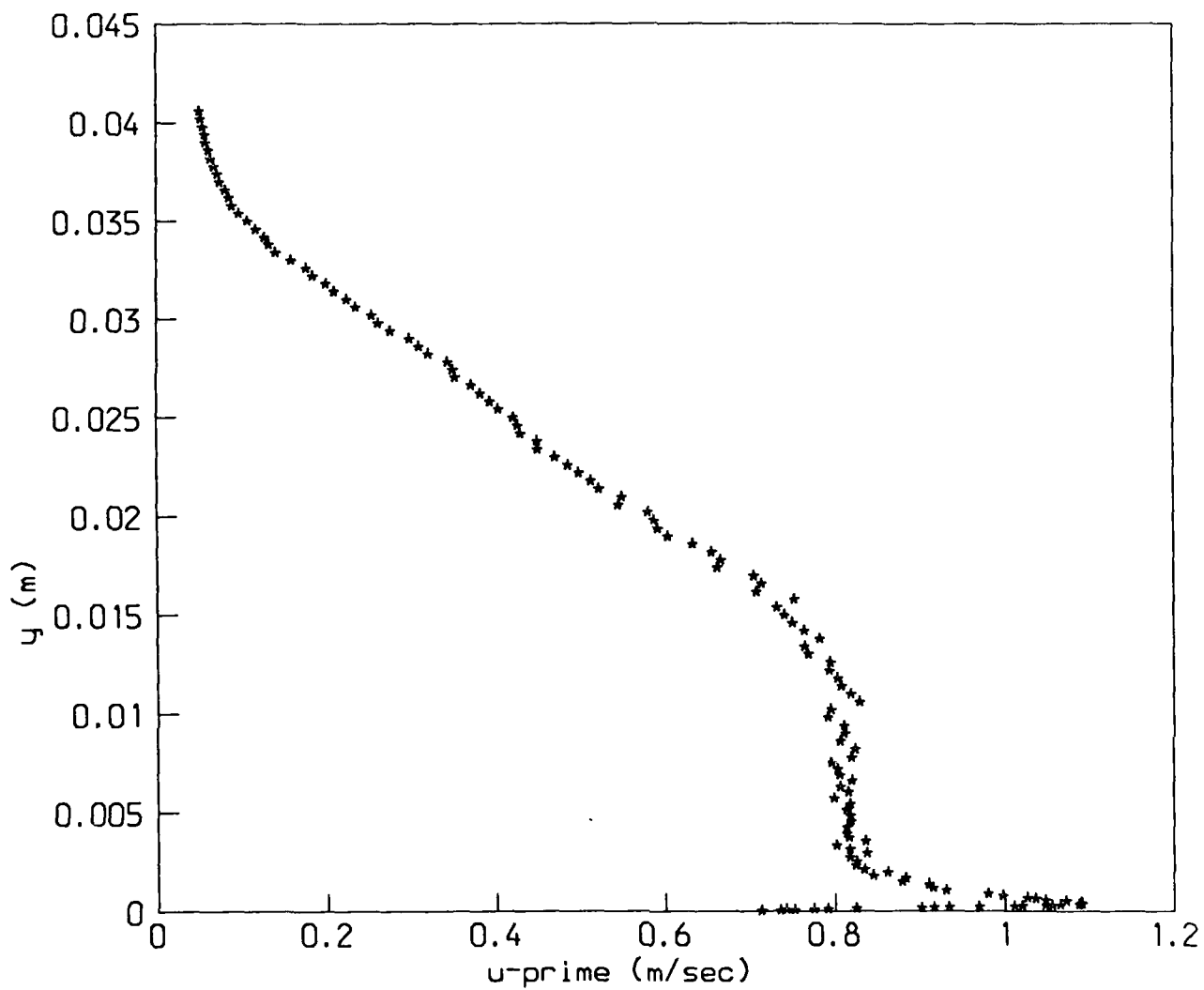


Figure 9f.: Manipulated Fluctuating Velocity Profile,  
6 - 1/8" cells LEBU,  $x_{LEBU} = 25in.$ ,  $U_{\infty} = 14 m/s.$

Fluctuating velocity

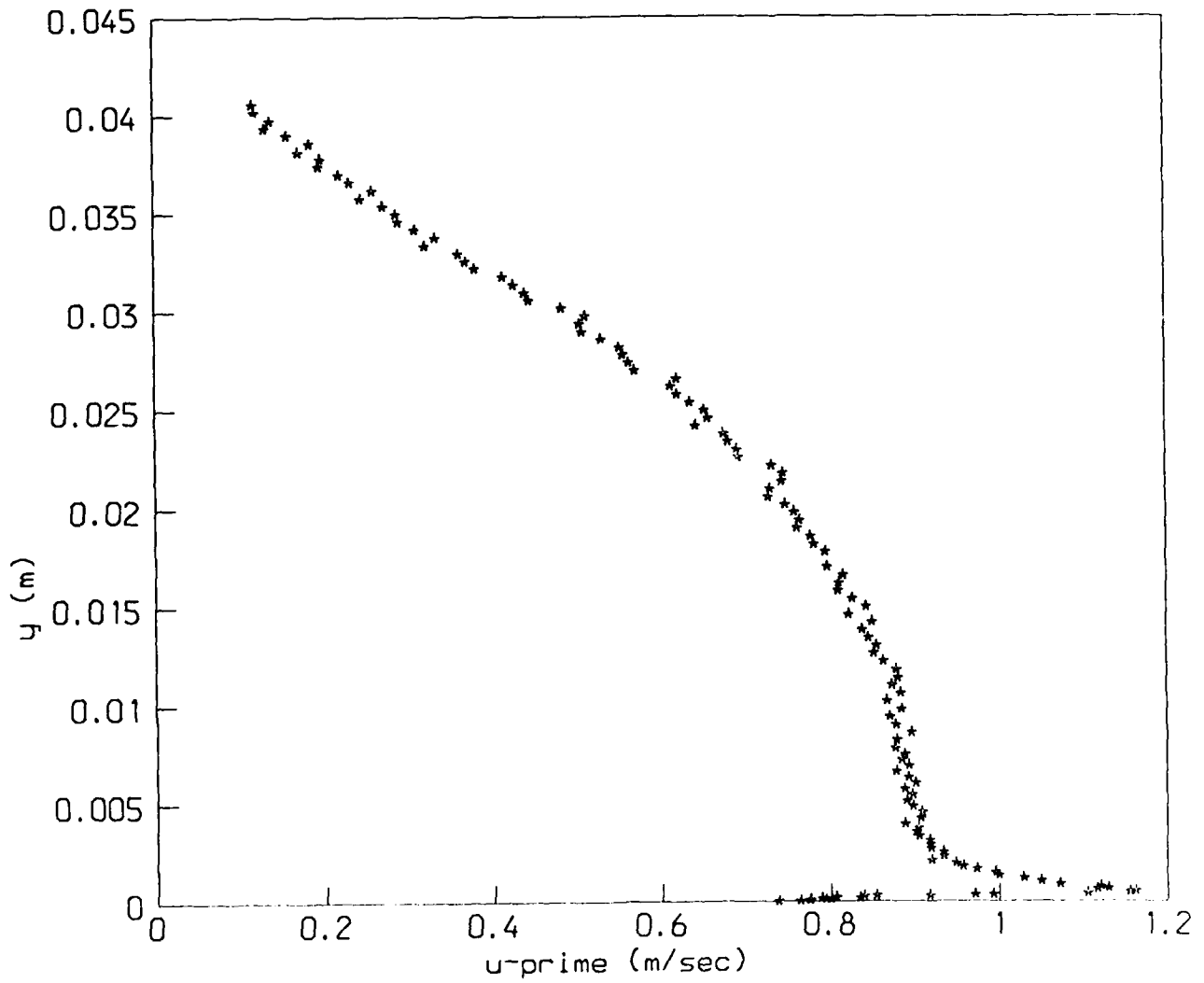


Figure 9g.: Manipulated Fluctuating Velocity Profile,  
6 - 1/8" cells LEBU,  $x_{LEBU} = 45in.$ ,  $U_{\infty} = 14 m/s.$

Reduction 3 - 1/8" LEBU

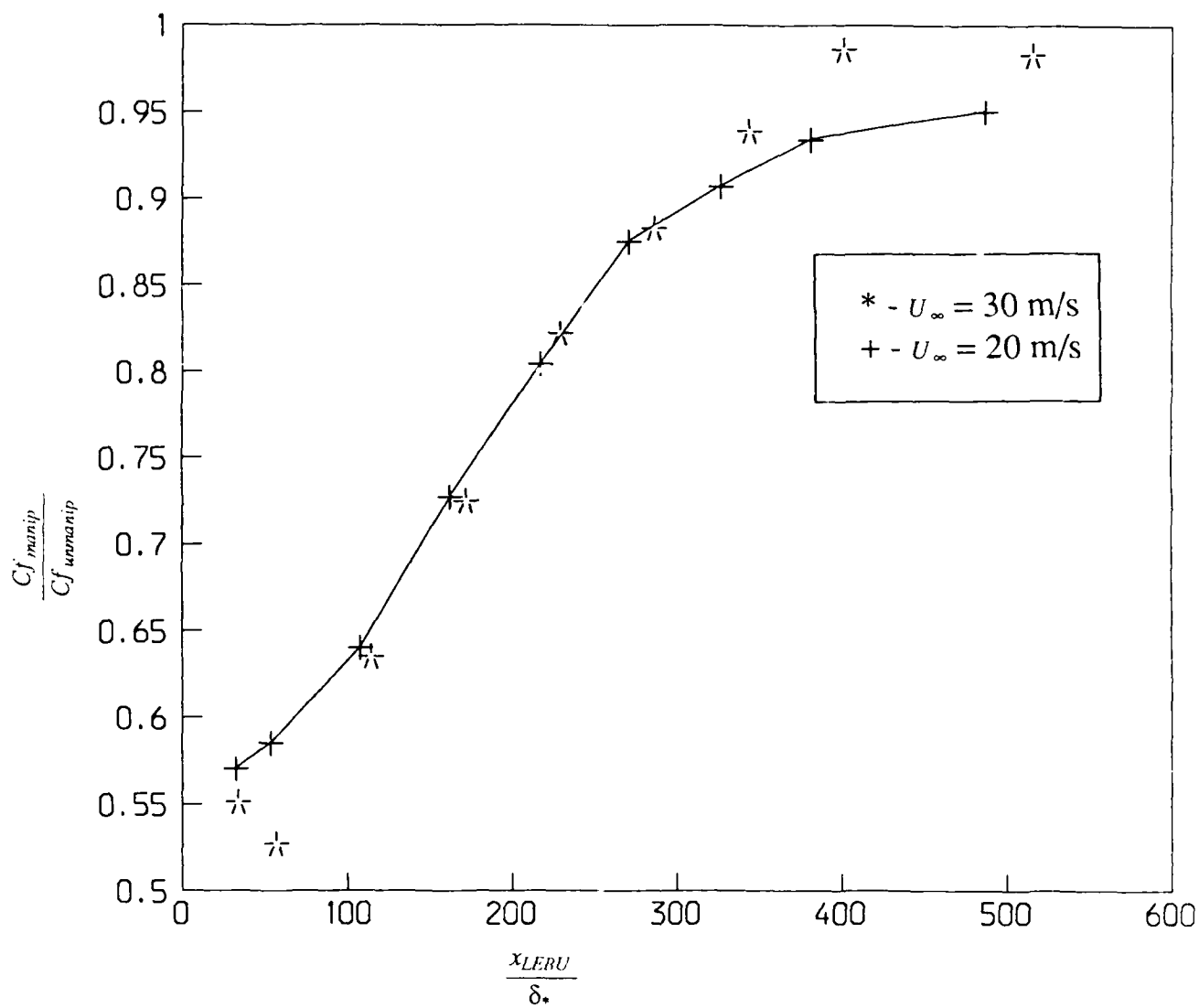


Figure 10a.: Skin Friction Reduction for a 3 - 1/8" cells LEBU.

Reduction 6 - 1/8" LEBU

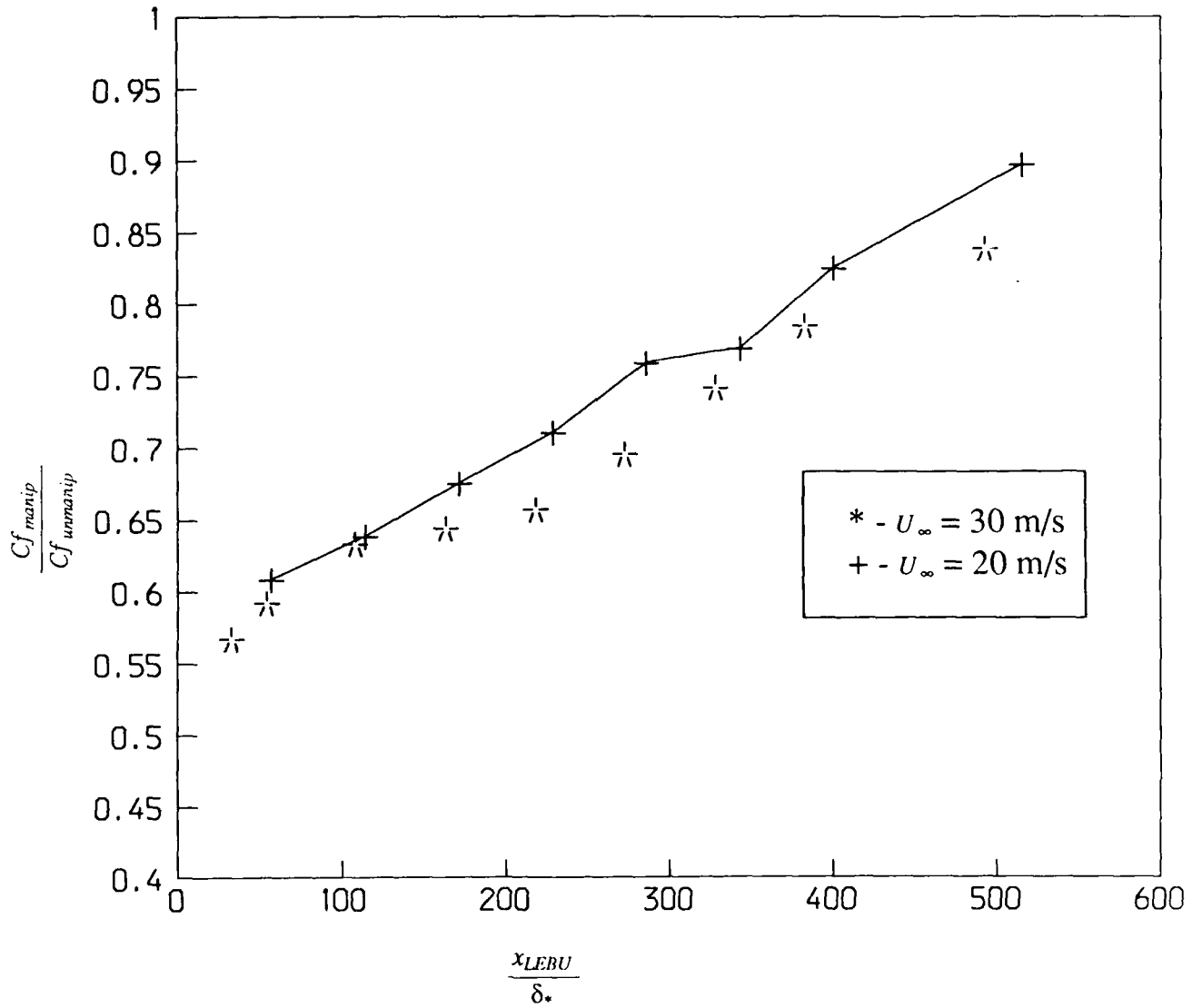


Figure 10b.: Skin Friction Reduction for a 6 - 1/8" cells LEBU.

Reduction 9 - 1/8" LEBU

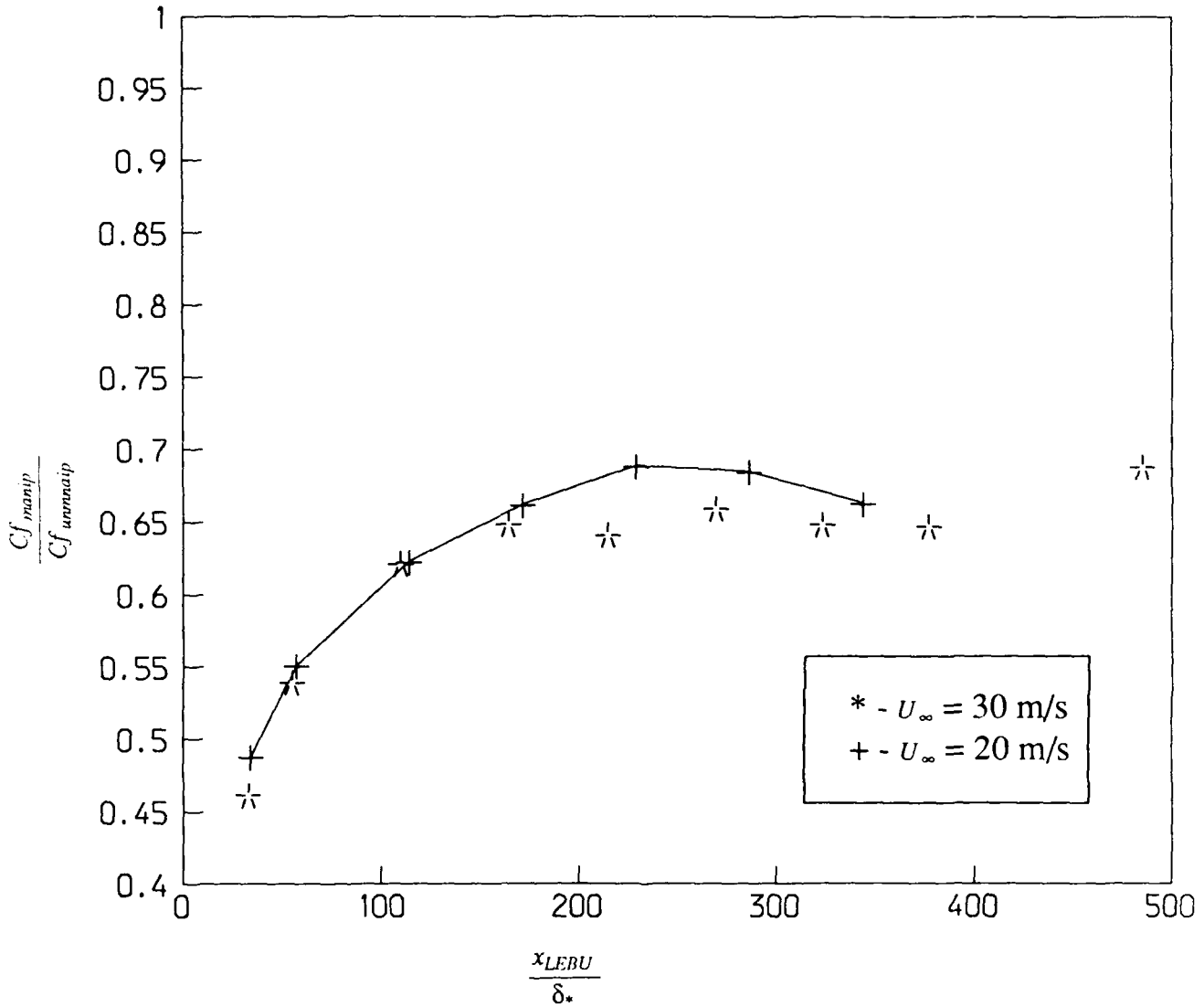


Figure 10c.: Skin Friction Reduction for a 9 - 1/8" cells LEBU.



Surface Fence Calibr

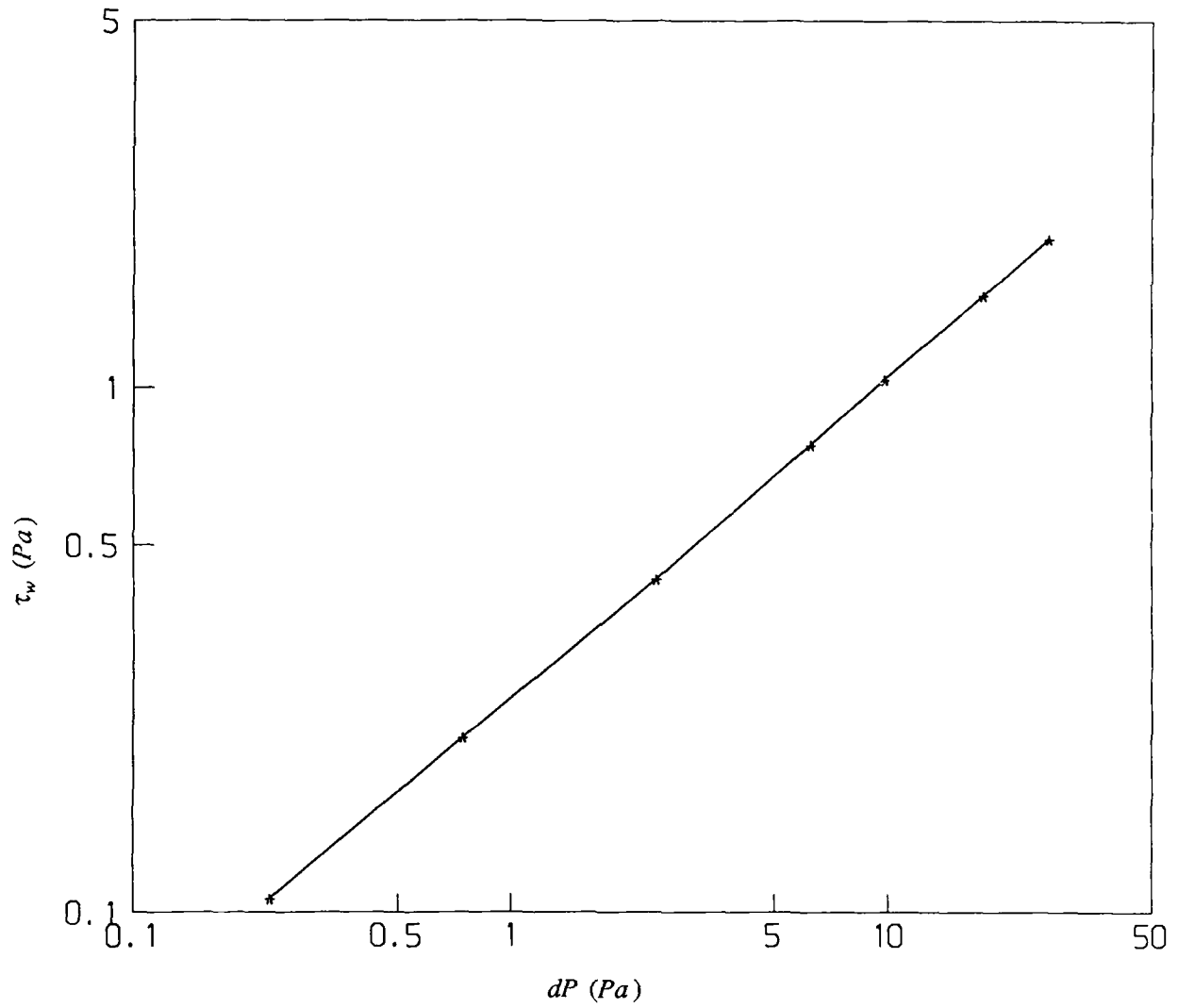


Figure 11: Sublayer Surface Fence Calibration Curve.

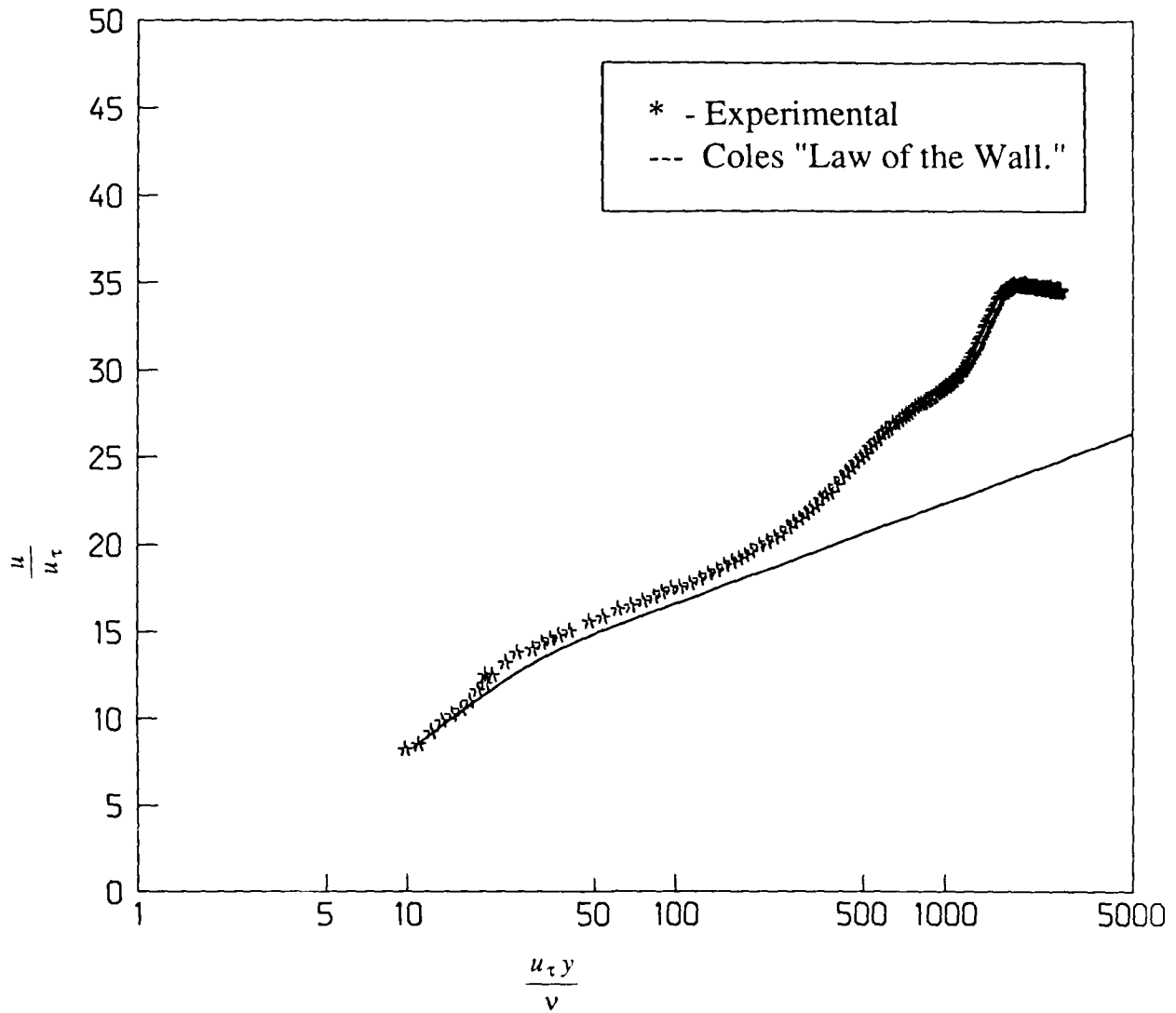


Figure 12a.: Manipulated Coles "Law of the Wall" Plot using surface fence  $\tau_w$ ,  $x_{LEBU} = 16.5in.$ ,  $U_\infty = 26 m/s.$

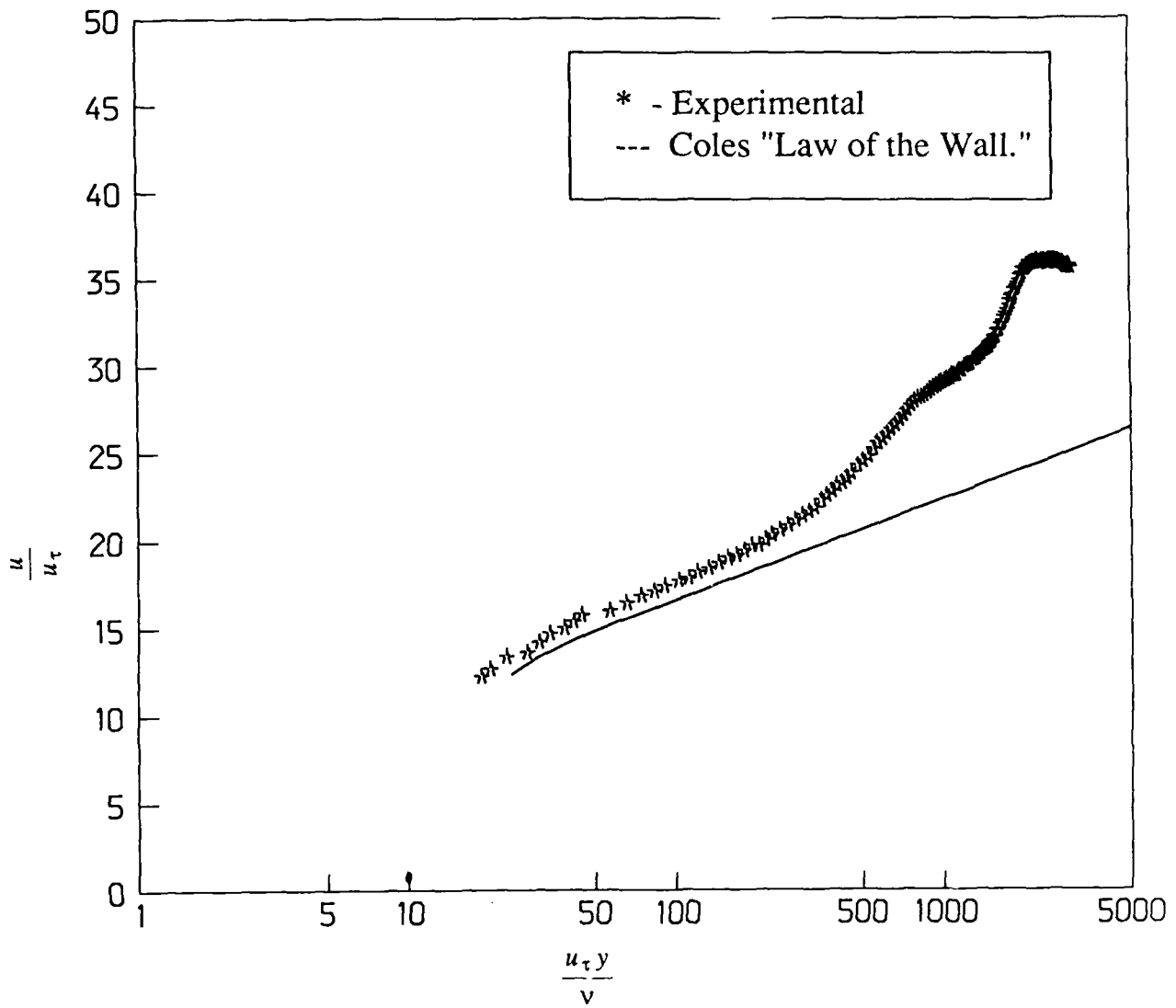


Figure 12b.: Manipulated Coles "Law of the Wall" Plot using surface fence  $\tau_w$ ,  $x_{LEBU} = 16.5in.$ ,  $U_\infty = 32 m/s.$

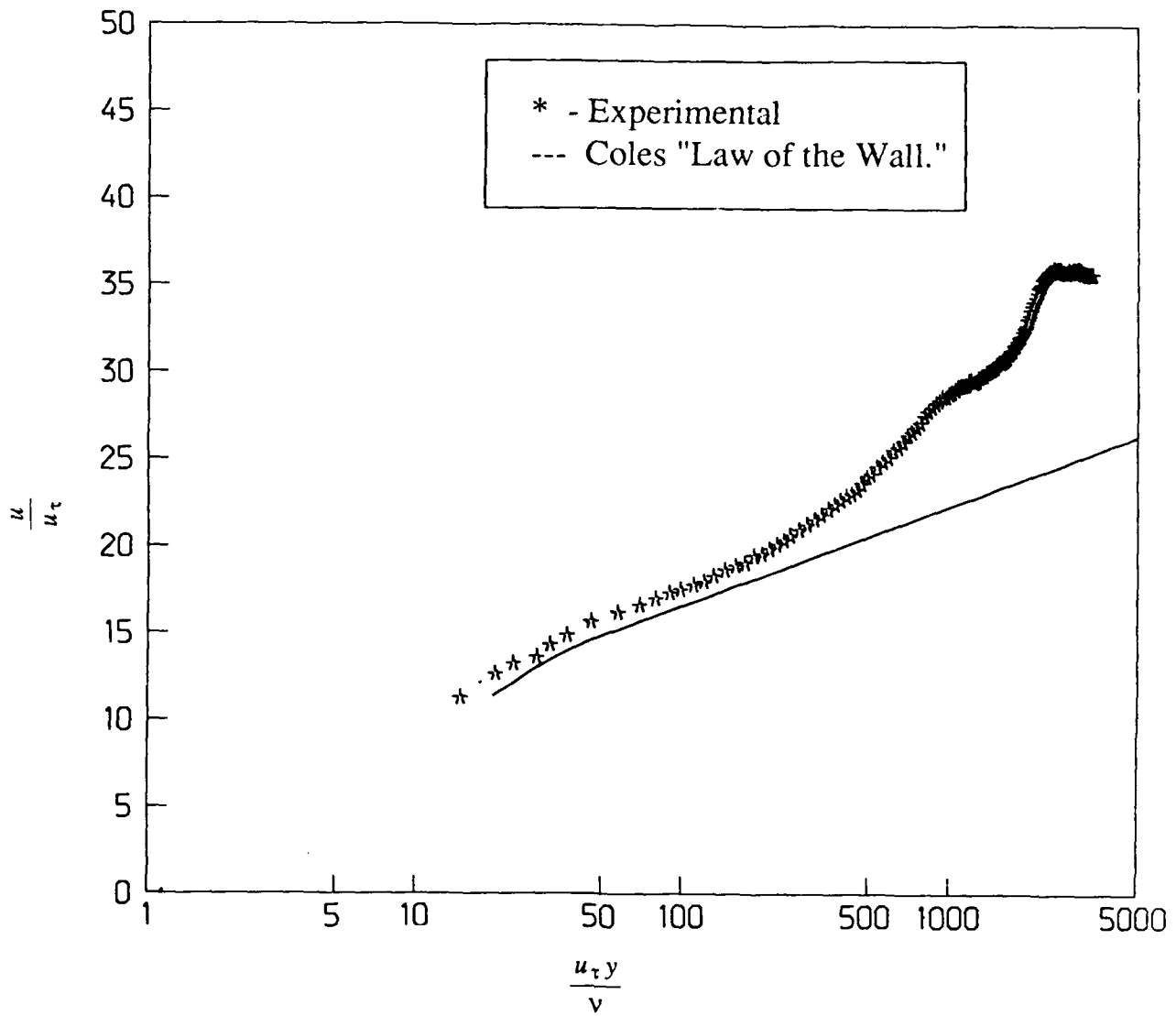


Figure 12c.: Manipulated Coles "Law of the Wall" Plot using surface fence  $\tau_w$ ,  $x_{LEBU} = 16.5in.$ ,  $U_\infty = 37 m/s$ .